Energy Conversion and Management 303 (2024) 118186

Contents lists available at ScienceDirect

Energy Conversion and Management

journal homepage: www.elsevier.com/locate/enconman

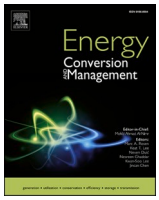

Research Paper

Reducing the environmental impact of international aviation through sustainable aviation fuel with integrated carbon capture and storage

Alberto Almena [a,b,*], Regina Siu [b], Katie Chong [b], Patricia Thornley [b], Mirjam Röder [b]

[a] Department of Chemical Engineering, University of Salamanca, Spain, Address
[b] Energy & Bioproducts Research Institute, College for Engineering & Physical Science, Aston University, Aston Triangle, Birmingham, B4 7ET, United Kingdom

ARTICLE INFO

Keywords:
Decarbonisation
Aviation
Sustainable Aviation Fuels
CCS
Lifecycle assessment
Net-negative emissions

ABSTRACT

Sustainable aviation fuels (SAFs) represent the short-term solution to reduce fossil carbon emissions from aviation. The Carbon Offsetting and Reduction Scheme for International Aviation (CORSIA) was globally adopted to foster and make SAFs production economically competitive. Fischer-Tropsch synthetic paraffinic kerosene (FT-SPK) produced from forest residue is a promising CORSIA-eligible fuel. FT conversion pathway permits the integration of carbon capture and storage (CCS) technology, which provides additional carbon offsetting capacities. The FT-SPK with CCS process was modelled to conduct a comprehensive analysis of the conversion pathway. Life-cycle assessment (LCA) with a well-to-wake approach was performed to quantify the SAF's carbon footprint considering both biogenic and fossil carbon dynamics. Results showed that 0.09 kg FT-SPK per kg of dry biomass could be produced, together with other hydrocarbon products. Well-to-wake fossil emissions scored 21.6 gCO_2e per MJ of FT-SPK utilised. When considering fossil and biogenic carbon dynamics, a negative carbon flux (-20.0 gCO_2eMJ^{-1}) from the atmosphere to permanent storage was generated. However, FT-SPK is limited to a 50 %mass blend with conventional Jet A/A1 fuel. Using the certified blend reduced Jet A/A1 fossil emissions in a 37 %, and the net carbon flux resulted positive (30.9 $gCO2eMJ^{-1}$). Sensitivity to variations in process assumptions was investigated. The lifecycle fossil-emissions reported in this study resulted 49 % higher than the CORSIA default value for FT-SPK. In a UK framework, only 0.7 % of aviation fuel demand could be covered using national resources, but the emission reduction goal in aviation targeted for 2037 could be satisfied when considering CCS.

1. Introduction

International commercial aviation provides the only rapid worldwide transportation network. The International Civil Aviation Organization (ICAO) estimated the number of passengers to be about 4.5 billion in 2019, equal to 8,686 billion revenue passenger kilometres (RPK) [1]. International aviation passengers have almost quadrupled since 1990 [2]. Only the existing mobility limitations due to the COVID-19 pandemic caused air traffic activity to fall by 66 % in 2020 [3] and 58 % in 2021 [4] compared to 2019 RPK levels. However, those effects were only temporary. Global air traffic is projected to increase between 4.3 % and 4.6 % annually in RPK compared to pre-pandemic values [4].

The strong reliance of aviation industry on petroleum-based liquid fuels, and the ongoing surge in demand, has led to a relentless growth in the GHG emissions generated by this sector [5,6]. Globally, aviation was responsible for 915 Mt of CO_2 in 2019 [7]. This is approximately 2 % of the total global anthropogenic CO_2 emissions, close to twice as much as the total emissions of the UK. However, if no action is taken, international aviation is forecasted to become the second-largest emitter by 2050 due to the continuous rise in air transport demand and the emissions reduction achieved in other sectors undergoing decarbonization efforts [8].

Many countries, including the United Kingdom, have committed to climate change mitigation by shaping trajectories towards a net-zero emission scenario that is targeted to be a reality by 2050 [10,11]. In 2019, the UK reported 40 % reduction in net GHG emissions when compared to 1990 levels [9]. Fig. 1 (a) shows the sectors sorted by GHG emissions contribution, including their emissions levels in 1990. Fig. 1 (b) indicates the percentage change in emissions for that period. While some sectors, such as waste disposal, energy (electricity and heat) supply and industrial processes, have started to decarbonize, international aviation has had the largest percentage growth in emissions (139 %). This trend was only disrupted by the COVID-19 lockdown measures.

* Corresponding author.
E-mail address: almena@usal.es (A. Almena).

https://doi.org/10.1016/j.enconman.2024.118186
Received 21 November 2023; Received in revised form 4 February 2024; Accepted 5 February 2024
Available online 14 February 2024

Nomenclature

Lowercase

odt	oven dry tonnes
p.a.	per annum

Uppercase

ASF	Anderson-Shulz-Flory
ASTM	American Society for Testing and Materials
ASU	air separation unit
B	carbon balance
BTX	benzene, toluene, and xylene
CAEP	Committee on Aviation Environmental Protection
CCGT	Combined cycle gas turbine
CCS	carbon capture and storage
CDR	Carbon dioxide removal
CEF	CORSIA-eligible fuels
CORSIA	Carbon Offsetting and Reduction Scheme for International Aviation
DEPG	Dimethyl ether polyethylene glycol
F	specific carbon mass flow (g CO2e MJ SAF^{-1})
FT	Fischer-Tropsch
GHG	greenhouse gas
GREET	Greenhouse Gases, Regulated Emission and Energy use in Technology
HC	hydrocarbon
IATA	International Air Transport Association
ICAO	International Civil Aviation Organization
ILCD	International Reference Life Cycle Data System
IPK	isoparaffinic kerosene
IRA	Inflation Reduction Act
ISO	International Organization for Standardization
JRC	Joint Research Center European Commission
LCA	lifecycle analysis
LCIA	lifecycle impact assessment
LHV	low heating value (MJ kg^{-1})
LS_f	lifecycle emissions value (gCO_2e/MJ)
LTFT	low temperature Fischer-Tropsch
MIT	Massachusetts Institute of Technology
NDC	nationally determined contribution
NE	net emissions
RPK	revenue passenger kilometres
SAF	sustainable aviation fuel
SPA	solid phosphoric acid
SPK	synthetic paraffinic kerosene
UK	United Kingdom
US	United States
WGS	water gas shift

Subscripts

AO	aircraft operation
BS	biological sequestration
BSC	biomass supply chain
CCSi	carbon capture and storage infrastructure
CS	stored carbon
CT	conversion technology
e	equivalents
JA1	jet A1 supply chain
out	outlet
raw	unprocessed material
torr	torrefied
TOT	total

The International Air Transport Association (IATA) committed in 2009 to approach reducing emissions by setting three main goals as illustrated in Fig. 2: improve fuel efficiency by 1.5 % annually to 2020, cap net emissions through carbon–neutral growth from 2020 and halve CO_2 emissions by 2050 taking 2005 data as a reference [12].

Progress in fuel efficiency has been made. The average fuel consumption decreased by 24 % on a fuel passenger^{-1} km^{-1} basis between 2005 and 2017 [15]. A myriad of studies is focused on improving aeroplane fuel efficiency. Evolutionary aircraft technologies try to innovate the current tube-and-wing aircraft with jet fuel-powered turbofan engines to improve aerodynamics [16,17], using new jet engine architectures [18,19] or including advanced aircraft systems

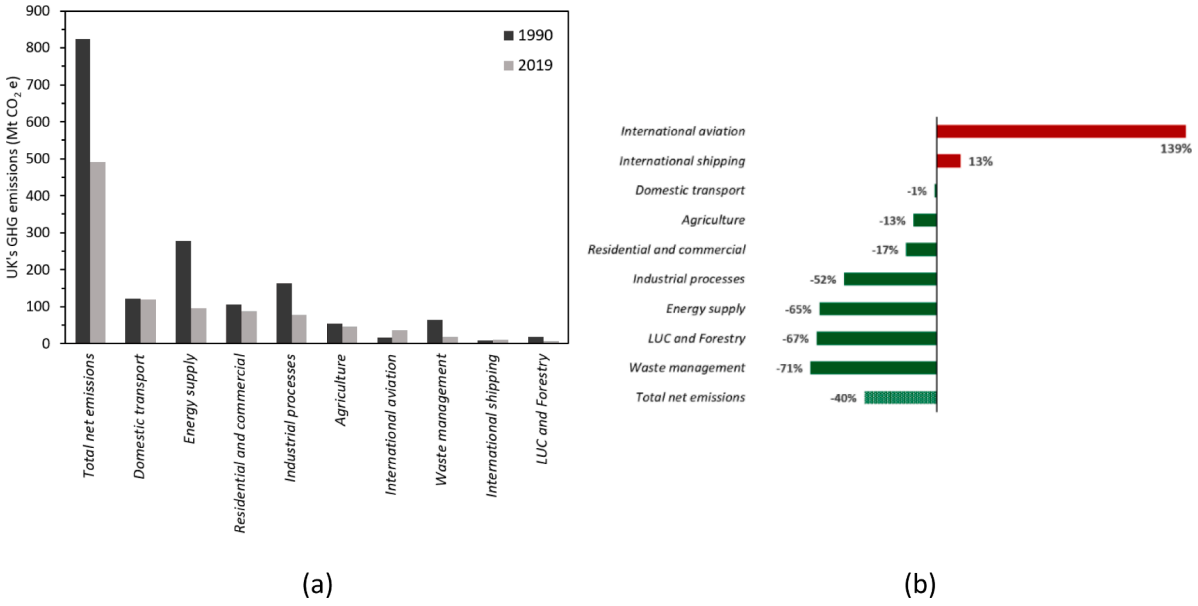

Fig. 1. Nationally determined contribution (NDC) of the UK by sector, reported for the reference year (1990) and the latest year reported (2019), in (a) absolute emissions by sector in 1990 (black) and 2019 (grey) and (b) percentage change of each sector between 1990 and 2019 [9]

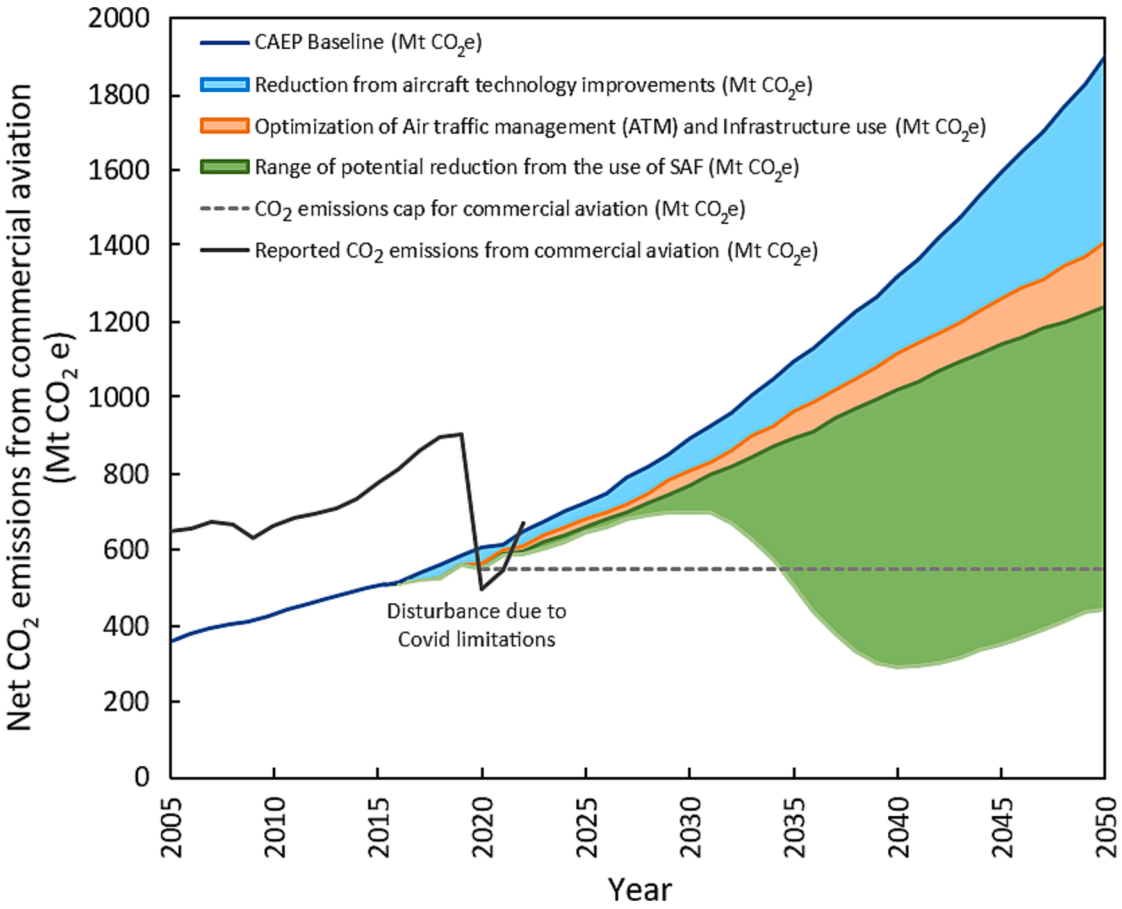

Fig. 2. Net emissions from commercial aviation [13] and international aviation. The estimated reduction in CO2 emission in international aviation (long-haul flights) is shown in coloured areas [14].

[20,21]. These technologies are expected to reach a 30 % improvement in fuel efficiency by 2030, when compared to 2005 numbers. Beyond such innovations, efficiency improvements are likely to plateau [22]. This reduction is insufficient to accomplish the 2050 goal set for aviation. Aircraft technology research investigates alternatives to conventional aircraft that could bring major emission reductions in the long term, such as innovative airframe designs [23,24], revolutionary materials [25], improved fuel additives [26] and fuel formulation [27], or novel jet propulsion technologies [28]. In addition, upgraded operational efficiency can reduce fuel consumption while improving airline economy [29].

To rapidly transition to low-carbon aviation, finding energy vectors that can substitute conventional fossil-based aviation fuels is essential. Kerosene, the conventional fuel used in aviation, is produced from the distillation of crude oil. Jet fuel is composed of C_8 – C_{16} hydrocarbons, alkanes, *iso*-alkanes, naphthenic or naphthenic derivatives and aromatic compounds, providing the properties required to operate a jet engine under the aircraft's changing conditions [30]. The aviation industry needs a short-term drop-in fuel solution to ensure the initial compatibility of alternative fuels with the current engines, aircraft fleet and fuel distribution systems.

Globally, about 60 % of CO_2 emissions from civil aviation are produced by aircrafts with a gross take-off mass above 45 t and operating at average stage lengths above 6,500 km [31]. This makes long-haul flights the main emitters of the aviation sector. Similarly, the UK reports 60 % of the UK's aviation emissions from flights with ranges above 5,000 km [8]. Carbon-free alternatives to conventional jet engines, namely electric (batteries), hydrogen or ammonia propulsion, are restricted by their inferior energy content per unit mass, showing limitations on take-off weight and maximum range [32,33]. Fully operational aircrafts using these technologies are not expected to become feasible alternatives for at least 25 years [34–37]. Additionally, nuclear and/or renewable electricity generation capacities would need to increase significantly, either to operate turboelectric engines or to produce green hydrogen, so that the CO_2 emissions generated by the alternative technologies do not outscore fossil kerosene operation [31].

Therefore, as shown in Fig. 2, the largest contribution to the decarbonisation of commercial aviation in the short to medium term is expected from using sustainable aviation fuels (SAFs), such as biofuels and e-fuels [38–40]. Aviation biofuels are biomass-derived synthetic paraffinic kerosene (SPK) suitable to be used directly or blended with conventional fuel. Multiple technologies have been investigated to produce SAF from a great number of feedstocks [41–43]. It is assumed that the emissions over the fuel lifecycle can be reduced when produced from sustainably sourced biomass. Besides, advanced aviation biofuels are likely to have low sulphur content, low tailpipe emissions, high thermal stability, good cold flow properties and show compatibility while achieving an enhanced performance on conventional engines. SAFs utilisation can save over 70 % of CO_2 emissions on a lifecycle basis and support net-zero targets when carbon dioxide removal technologies are integrated into the production process [44]. Thus, conventional aircraft comprising jet combustion engines fuelled with biobased SAF, improved fuel efficiency, and optimised flight operation can represent the most promising short-term strategy to achieve emission savings for long-haul flights.

Nevertheless, policy intervention is required to incentivise aviation stakeholders to reduce air transport's carbon footprint. The range of cost for SAFs is currently wide and technology-dependant, which can quadruple the cost of Jet A fuel [45]. Since fuel purchase constitutes between 20 % and 30 % of an airline's total expenditure [46], closing

the price gap is needed not to compromise economic performance. In this regard, the US incorporated a subsidy programme for SAFs in the recent Inflation Reduction Act (IRA) introduced a $1.25 tax credit per gallon of SAF reducing 50 % lifecycle emissions compared to fossil jet fuel [47]. Furthermore, global market-based measures have been introduced, including GHG emission caps, trading systems, and offsetting schemes [48]. ICAO recently promoted the Carbon Offsetting and Reduction Scheme for International Aviation (CORSIA), Which aims to freeze net emissions to 2020 levels [14]. As a contracting state of ICAO, the UK has committed to implementing CORSIA. In addition to these schemes, national governments are also promoting policies to cap emissions of both domestic and international flights. For example, the UK's Sixth Carbon Budget commits to reducing the UK's emissions to 78 % below the 1990 level by 2035, for the first time, including international aviation and shipping emissions [49].

One of the methods for an airline to claim emissions reduction is using CORSIA-eligible fuels (CEF). To be CORSIA eligible, the fuel must be derived from sustainable feedstocks approved by the Committee on Aviation Environmental Protection (CAEP) and be produced using fuel conversion pathways accepted by the American Society for Testing and Materials (ASTM). These requirements make CEF and SAF similar concepts. The CORSIA program lists default lifecycle emissions values for any CEF [50]. The CORSIA pilot phase started with voluntary participation in 2021 and becomes a mandatory scheme for most states in 2027 [51].

The aim of this research was to investigate the Fischer-Tropsch Hydroprocessed Synthesized Paraffinic Kerosene (FT-SPK) pathway, an ASTM-certified route to produce jet fuel from renewable and non-renewable feedstocks and catalogued as CEF when waste wood is used as feedstock. CORSIA default lifecycle emissions values for this route do not consider carbon capture and storage technology (CCS) as part of the process. This approach's novelty was challenging the common assumption for biogenic carbon accounting as climate neutral and include it in the assessment. This will allow to assess and quantify the additional environmental impact mitigation originated from integrating CCS in the FT-SPK production process, which creates a negative carbon flow from the atmosphere to a geological storage [52]. Process modelling and lifecycle assessment methodologies were implemented to evaluate process performance accurately and monitor carbon dynamics along the entire SAF supply chain. With this, the objectives of this paper are to:

- Using carbon capture and storage technology, evaluate the theoretical performance and compute the lifecycle emissions of converting forest residues to sustainable aviation fuel.
- Identify key parameters from the process and assess their effect on the lifecycle emissions score.
- Compare the results from this study to the CORSIA default lifecycle emissions for airlines to certificate emission reduction by using this type of fuel.
- Make policy recommendations for decarbonising international commercial aviation.

The UK's Royal Society has recently brought attention to a lack of comprehensive assessment in determining the carbon balance linked to the production of aviation fuel from biomass [45]. Techno-economic and environmental assessments for e-fuels and oil-to-jet technologies can be found in literature [40,53–55]. However, to the best of authors' knowledge, this is the first work developing a complete and detailed model in a validated and robust process simulation software (Aspen Plus) for the FT-SPK route for SAF production from wooden residue, which includes feedstock pretreatment, biomass-conversion process, carbon capture and storage, upgrading stages, SAF yield maximization processes and auxiliary unit operations. The work examined the underpinning engineering process/steps, and integrated a comprehensive lifecycle assessment, with a well-to-wake approach, founded on the developed process modelling and an aircraft operation model to estimate the produced fuel performance in a jet turbine. This research pretends to be transparent and make traceable any impact contribution to the SAF final score, so that the recommendations and conclusions generated from this study are based on a strong scientific methodology and involve high confidence.

2. Materials and methods

2.1. Assessment methods

A whole supply chain approach was taken, assessing all relevant lifecycle stages as shown in Fig. 3. This included supply chain activities from biomass growth to SAF consumption during aircraft operation, considering carbon fluxes from fossil and biogenic sources. This is essential when considering incorporating carbon dioxide removal (CDR) technologies in the SAF production process to capture some of the CO_2 and reduce aviation's emission impact. The different supply chain stages included forest growth and management, wood residue sourcing, feedstock pre-treatment, FT conversion process, fuel upgrading, aircraft operation, CO_2 capture and storage/use, and any transportation required to connect consecutive supply chain stages.

The applied methodology combined process modelling and lifecycle assessment (LCA). Feedstock pre-treatment and SAF production via FT-synthesis with carbon capture were modelled using ASPEN Plus. The designed model allowed a detailed analysis of such a complex process, thus enabling sensitivity analysis capabilities and optimisation potential. The resulting mass and energy balances, biomass-to-SAF yield, CO_2 removal fraction and resulting energy penalty, and heat and power demand defined the whole process. Process modelling outputs were incorporated into the encompassing LCA. The impact of technical parameters and process configurations on the SAF's net emissions score was evaluated to test sensitivity on the carbon emission reduction achieved for international aviation.

A detailed estimation of the economic performance of this process was beyond the scope of the present work. However, the cost for SAF through the chosen technology pathway was compiled from the literature and accounted for in the final recommendations for decarbonising international aviation.

2.2. Biomass feedstock

Biomass captures CO2 from the atmosphere as it grows. Utilizing sustainable biomass as the feedstock for FT synthesis has the potential to diminish the emission impact of SAF. Promising sources for efficient thermochemical conversion to SAF include woody and herbaceous perennials such as poplar, miscanthus, and switchgrass, as well as woody biomass residues like forestry and sawmill by-products [38,56,57]. In this study, low-quality wood, forestry, and sawmill residues were considered suitable feedstocks for SAF production.

The availability of small, low-quality roundwood, sustainably sourced forestry residues and sawmill residues is estimated between 2.7 and 3.3. Mt p.a in the UK [52,58]. Considering possible other uses for the woody feedstock, it is projected that between 1.0 and 2.0 Mt p.a of these resources could be available for bioenergy. The use of accessible residue would minimise the land-use change penalty from this activity.

In the UK, conifers cover around 51 % of the woodland area. Pine species (Sitka spruce, Scots pine and Larches) account for 80 % of the UK's conifers [59]. Thus, pine wood is assumed as feedstock for SAF production, and Table 1 shows the feedstock characterisation.

2.3. Description of the SAF process

This section describes the whole biomass-to-SAF conversion process via the Fischer-Tropsch pathway. The conversion includes the feedstock pre-treatment through torrefaction, followed by gasification, syngas

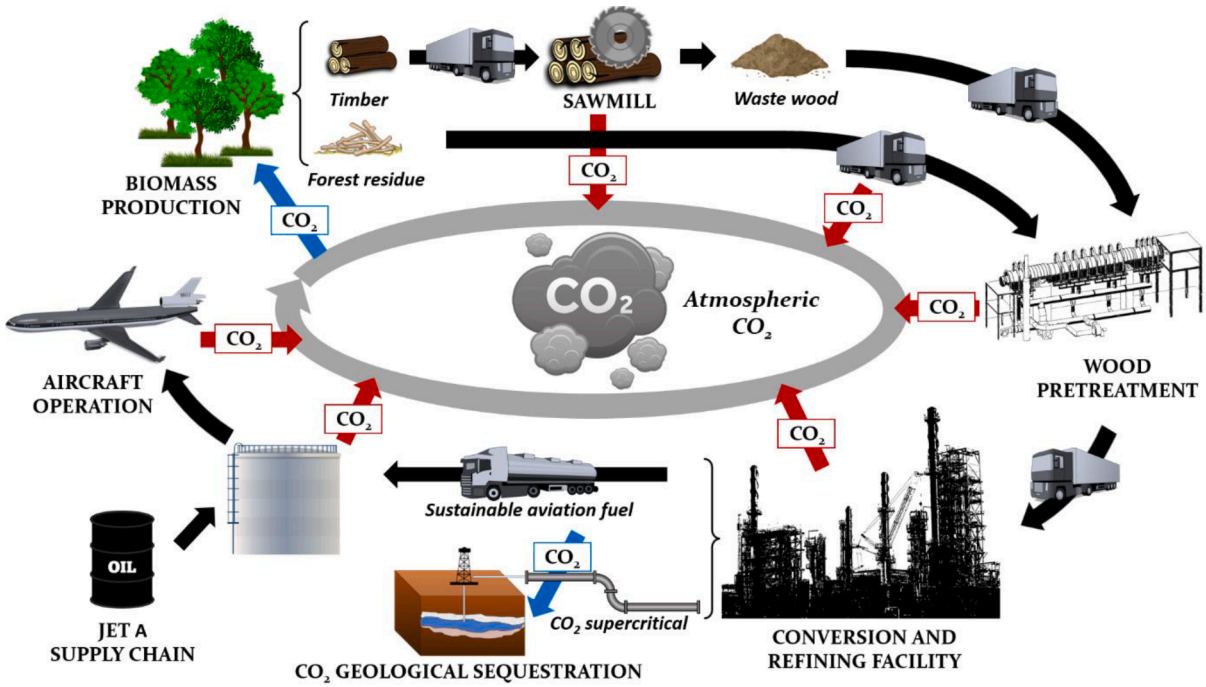

Fig. 3. SAF supply chain. The resulting balance of CO2 sinks (blue arrow) and sources (red arrow) will determine the net GHG emissions balance of the system.

Table 1
Proximate and ultimate analysis for raw and torrefied pine wood.

	Pinewood [60,61]	Torrefied pinewood [62,63]
Moisture	48.50[64]	7.47
Volatile content (VC)	85.47	56.87
Fixed carbon	14.23	42.77
Ash	0.30	0.36
C	47.95	53.12
H	6.03	7.09
N	0.72	0.86
S	0.00	0.00
O (difference)	45.00	38.57
Low heating value (MJ kg^{-1}, dry basis)	16.95	20.34

cleaning and conditioning, CO_2 absorption, FT synthesis, biocrude fractionation and upgrading and auxiliary energy generation. Fig. 4 shows the unit operations of the designed process. A detailed flowchart can be found in the Supplementary material (Figs. S1–S12).

The plant capacity considered for this study had a biomass input of 145 t h^{-1}. Therefore, continuous operation of this plant during a year (8,760 h $year^{-1}$) would consume 1.27 Mt p.a. of feedstock. Hence enough domestic feedstock would be available if directed to SAF production at assumed capacity.

2.3.1. Biomass pre-treatment

Wood residues need to be dried and milled before gasification. Pine wood's average relative moisture content is 48.5 mass % [64]. At this condition, the feedstock needs to be dried to reduce moisture to a maximum of 20 mass %, but preferably 15 to 10 mass % to make it a suitable feedstock for gasification [65,66]. Commonly, residues are not dried [67], which implies that pre-treatment is necessary before the FT process.

The particle size of wood must also be reduced to achieve an effective thermochemical conversion. Depending on the technology selected for gasification, wood chips are broken down to a maximum particle size. Entrained flow gasification was considered, for which biomass needs to be pulverised before being fed into the gasifier [68]. Hence particles must be smaller than 100 μm. A vibration mill was selected to reach that optimal particle size [69].

To save energy at powdering and improve gasification performance, the wood chips are pre-dried in a rotary kiln at 120 °C and torrefied in a multiple hearth furnace at 275 °C [70,71]. Torrefied wood significantly reduces the energy consumption for grinding and pulverisation, requiring only 20 % of the energy compared to dry wood milling [72]. Two closed water cycles for indirect heating using superheated steam at pre-drying (1 bar) and torrefaction (6 bar) were assumed to reduce the water footprint of the process. The heat integration allowed to use of excess heat produced downstream at the FT reactor to supply the torrefaction stage. Some of the separated CO_2 at downstream stages was used as carrier gas.

Pre-drying reduced the moisture content of biomass to 18 %. During torrefaction, water (70 %) and volatiles (26 %) mass loss occurred, altering the chemical composition of wood[59]. The characterisation of torrefied pine wood is shown in Table 1. The composition of the resulting torrefaction gas was consulted in literature and compiled in Table 2.

2.3.2. Thermochemical conversion: Biomass gasification

Gasification converts biomass to syngas, which is the precursor for FT synthesis. Entrained flow gasification is a very efficient technology for biomass gasification, suitable to process biomass with high conversion rates of up to 99 % [74]. The considered plant size [66], the feedstock input is above 1,600 odt day^{-1}. Entrained flow gasifiers operate at high temperature and pressure conditions, ranging between 1,250 – 1,600 °C and 2.0 – 8.5 MPa. These extreme operating conditions allow clean and tar-free syngas production [75]. Oxygen is employed as a gasification agent to reach those high temperatures and reduce downstream equipment sizes at an equivalence ratio of 0.3 [64]. Soot and ash are undesired by-products of entrained flow biomass gasification that melt and cause fouling and corrosion [74,76,77]. Therefore, a water-cooling system was considered, consisting of a first radiation screen to recover heat and subsequent water quenching to solidify the ash and soot sludge recovered at the bottom of the equipment. Particles from the water-saturated and tar-free syngas leaving the gasifier are removed in a ceramic filter. The syngas is then sent to the conditioning step. The

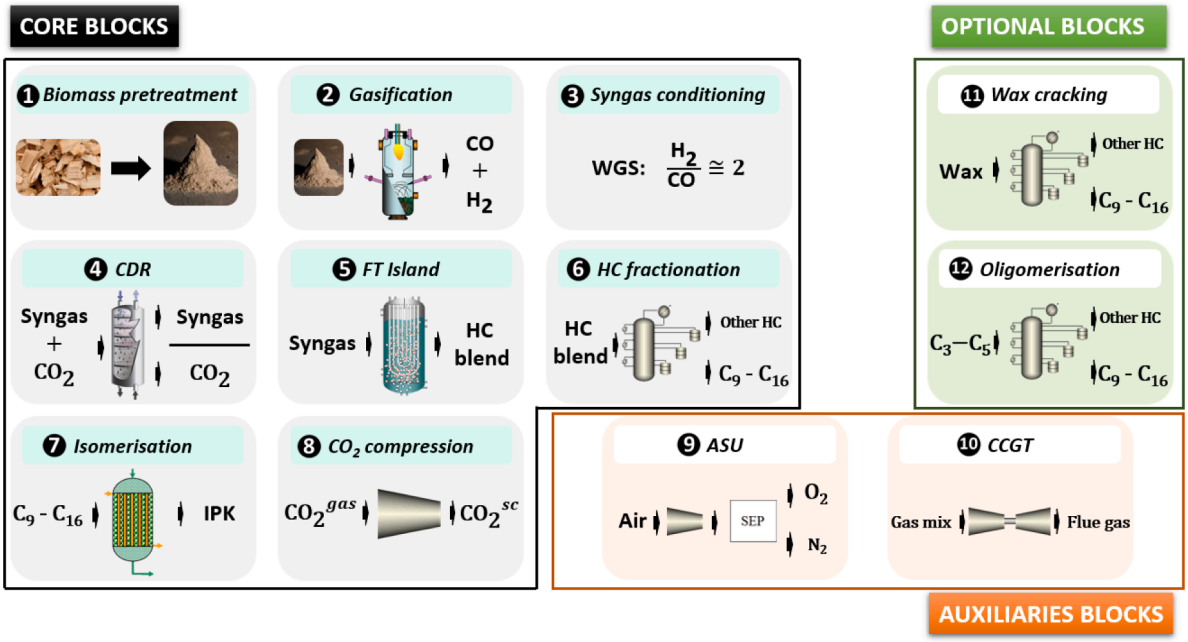

Fig. 4. Unit operations within the FT process for SAF production, including carbon dioxide removal.

Table 2
Gas mix composition of the output gas from biomass torrefaction.

Torrefaction gas mix	mol % [73]
H2O	63
O2	15
CO	11
CO_2	9
CH_4	2

following water gas shift (WGS) reaction occurs in a catalytic packed-bed reactor at 300 °C adjusted with the H2:CO mole ratio to 2:1 to satisfy FT synthesis optimal conditions [78].

2.3.3. Carbon dioxide removal unit

A commercially proven physical absorption technology is the Selexol process. Dimethyl ether polyethylene glycol (DEPG) is used as solvent for pre-combustion CO_2 capture to treat the high-pressure syngas [79]. This process can achieve up to 95 % carbon capture efficiency [80]. Physical absorption is based on Henrýs law. It depends on the CO_2 solubility in the solvent with no chemical reaction. The high pressure of input syngas facilitates subsequent non-thermal solvent regeneration [77]. Syngas is first cooled to ambient temperature, and the decanting water is removed before entering the absorption column. Countercurrent flow is implemented to improve the gas-solvent contact. The rich solvent from the column bottom is regenerated using two flash drums that regenerate the CO_2 with consecutive adiabatic expansions. The lean solvent is then pressurised and recycled back to the absorption column. Purge and make-up solvent flow is accounted for to avoid solvent saturation. The sulphur content of selected biomass is negligible. However, DEPG would absorb any sulphur from syngas if another type of biomass was used, thus preventing FT catalyst poisoning in the subsequent synthesis stage [81].

2.3.4. Fischer Tropsch island

The syngas exiting the CDR unit undergoes an FT reaction, i.e. a catalysed reductive polymerisation of carbon monoxide that produces straight-alkanes, ranging from methane to high-melting paraffins, as primary products [82]. Product distribution depends on the catalyst, the synthesis temperature, and the type of process employed [83]. A slurry bubble column reactor allowed great temperature control in a highly exothermic FT reaction [84,85]. The heat of the reaction is removed by water evaporation inside cooling pipes immersed in the slurry [86], enabling using that heat for other processes. A precipitated iron-based catalyst under low-temperature FT conditions and high pressure was selected to enhance the reaction yield to aviation fuel carbon range, i.e. C10–C14 [87]. A fraction of the light gases leaving the reactor is recycled to maximise HC production to achieve a carbon monoxide conversion of 0.9 [88]. The produced liquid FT hydrocarbon blend is then sent to the fractionation stage.

2.3.5. Refining and upgrading

The FT products must be further processed to reach aviation fuel specifications. A fractionated distillation column separates the biocrude into different compounds. One of the product fractions obtained is synthetic paraffinic kerosene since LTFT produces a highly paraffinic fuel with a very low or no aromatics content [89]. Unavoidable byproducts are also obtained, namely light gases (C1-C5), naphtha (C5-C9), diesel (C14-C20) and wax (>C20) fractions.

Light gases from the FT reactor and distillation column undergo an oligomerisation process to maximise the yield of SAF. A cryogenic separation (about −80 °C) is required to recover the C3-C5 fraction from the light gases. An auxiliary ethylene refrigeration system, combined with a turboexpander-compression train to reduce the energy input, is considered [90]. The C3-C5 fraction is recovered by distillation and sent to the oligomerisation reactor. A packed bed reactor with solid phosphoric acid (SPA) on kieselguhr as catalyst was selected to perform the reaction at 200 °C and 2.5 MPa [91]. The hydrocarbon (HC) product is highly branched with a high proportion of kerosene's range that is recovered in a fractionated distillation column [92,93].

The FT wax fraction underwent hydrocracking to produce an additional SAF stream and improve the economics of the Fischer–Tropsch technology [94]. A trickled-bed reactor using a bifunctional catalyst comprising platinum in a silico-alumina matrix was considered. This operates at 320 °C in a high-pressure hydrogen environment (3.5 MPa) [95]. Part of the excess hydrogen is recovered and recycled. High conversion for the wax feed (80 %) can result in a branched product with a major SAF length-chain fraction [96]. A final fractionated distillation column separates the hydrocarbon product blend obtained into the

different fuel fractions.

Adequate distillation range and degree of isomerization are essential for aviation fuel to achieve a low freezing point and optimal cold-flow properties during the cruise flight phase [94]. Synthetic paraffinic kerosene from FT synthesis enters the upgrading stage, a hydro isomerisation process that converts the predominantly linear hydrocarbons into branched isoparaffins suitable to operate aviation turbines (IPK). The feed stream comprising the previously obtained SAF product streams is mixed with hydrogen and heated to the reaction temperature. A fixed bed isomerisation reactor operates in a hydrogen once-through configuration at 250 °C and 2 MPa, with a sulphided Pt-ZrO2/Al2O3 catalyst [97]. At these conditions, isomerisation and hydrocracking reactions occur simultaneously [98]. A light gas stream is sent to a gas turbine, and the isomerised SAF stream is obtained as the final product.

2.3.6. Auxiliary blocks

An air separation unit (ASU) and a combined cycle gas turbine (CCGT) were included in the studied process. The ASU supplies the high-pressure oxygen stream required for the entrained flow gasification and the low-pressure oxygen needed for oxidizing the carbon monoxide and hydrogen unavoidably captured together with the CO_2 at the CDR unit.

The light gases obtained during the conversion process stages are mixed and used as fuel for a combined cycle CCGT [99]. The design of the turbine must be tailored to operate the gas mix. The unit produces electricity to cover part of the power demand from the process. Flue gases are vented into the atmosphere.

2.4. Process modelling

The complete FT process outlined above was modelled as a continuous stationary process in Aspen Plus. The overall aim of the process modelling was to accomplish a thermodynamic equilibrium calculation, which predicts the thermodynamic limits of the biomass conversion process. This is an approximation. The equipment's design was not included since equilibrium cannot be reached under normal operation. However, the process modelling can determine the components' formation, consumption and separation and set yield limits [100]. Aspen Plus was used to create a digital study. Material and energy balances were carried out using Aspen Plus capabilities, including accurately describing pure components' physical and chemical properties, complex mixtures, and rigorous unit procedure models [101]. The modelling was also supported with Fortran user block models when required. The process modelling allowed the evaluation of the plant's behaviour with various operating conditions and performance parameters. The Supplementary material contains both unit operation parameters and supporting codes in section S.1.

Raw pine wood entering the process has the composition compiled in Table 1. A rotary dryer and multiple heath furnaces were modelled as stoichiometric reactors. A Fortran block was implemented to calculate the conversion to achieve the final moisture content from drying. Torrefaction was modelled developing an empirical stoichiometric reaction (Eq. 1), that was obtained performing an atom balance based on literature data previously mentioned, i.e. raw and torrefied pine wood compositions (Table 1) [60–63], mass loss (moisture and volatiles) occurring, and generated torrefaction gas composition (Table 2) [73]. The gas stream produced was separated using flash units. At the same time, the auxiliary water/steam closed cycles were modelled using a combination of pump and heat exchangers.

$$Pine_{raw} \rightarrow 0.7420 Pine_{torr} + 0.0070 H_2O + 0.0016 O_2 + 0.0012 CO + 0.010 CO_2 + 0.0002 CH_4 \quad (1).$$

Gasification was modelled assuming that product gases from biomass devolatilization can be calculated from its elementary composition, i.e. ultimate analysis [56]. For this purpose, a yield reactor with a calculator block was used to decompose torrefied wood into ash, moisture and elementary components (C, H, O, N, S). Subsequently, an RGibbs unit calculates the Gibbs equilibrium, restricted to a temperature −10 K below the gasifier's temperature [77], to estimate the producer gas composition. To cool the syngas, a heat exchanger represents the water radiation section producing steam for drying/torrefaction. The water flow, added in a second heat exchanger representing the quench, was computed with a calculator block so that the heat removal from direct contact and water evaporation is enough to solidify the slag[102] and cool the gas to 300 °C. A Cyclone and a Sep block separate the solidified slag and the remaining particles from the gas. Then, an equilibrium reactor (REquil) modelled the WGS reactor, using a calculator block to compute the extra steam flow needed to reach an H_2O/ input ratio of 1:1 at the reactor to enhance the forward reaction to hydrogen [103,104].

The following stage is the CDR process. A RadFrac block model with neither condenser nor reboiler simulates the CO_2 absorption in DEPG with a solvent/CO_2 feed mole ratio above 2:1. A medium-pressure flash (1.1 MPa) and low-pressure flash (0.1 MPa) were used to expand the rich solvent and desorb the CO_2. The lean solvent was then recompressed and recycled. A small part of the CO and H_2 was also captured with the solvent and desorbed within the CO_2-rich stream. That stream was oxidized in combustion with oxygen to convert the present CO into CO_2. Then, four compression stages with intercooling and water decanting units were employed to reach the supercritical CO_2 state and have it ready to enter the pipe leading to geological storage [56].

The CO_2-free syngas was sent to the FT synthesis reactor. A calculator block (Excel based) computed the Anderson-Shulz-Flory (ASF) mathematical model and estimated the FT product distribution [90,105]. A Flash block separated gas and liquid product streams. The biocrude was later distilled using a series of distillation columns (RadFrac) to obtain the different fuel fractions.

The non-recycled FT gas product and the light gas fraction from distillation entered the oligomerisation stage. A compressor block first compresses the gas as the first stage of the turboexpander-compression train. Then, the compressed gas is first cooled in a multiple heat exchanger (MHEATX) with the cold gases produced downstream and subsequently in a heat exchanger representing the auxiliary ethylene refrigeration system. The power input of this system was calculated using the coefficient of performance reported in the literature [92]. Cold gas is then expanded in a turbine (COMP) for power recovery and distilled in a RadFrac to recover the C3-C5 hydrocarbons. The top stream was used at the MHEATX as the cold fluid, and the subsequent selective membrane separated the CO_2 from methane and ethane gases [106]. The separated CO_2 entered the compression block previously referred to. Finally, the light fuel gases were used to feed the gas turbine.

On the other hand, the C3-C5 recovered at the distillation bottom were heated to oligomerisation reaction conditions. A yield reactor (RYield) was employed to set the product distribution[95] and branching percentage[94] obtained from experimental studies. The fractions of the hydrocarbon product stream were separated in another fractionated distillation. Similarly, wax cracking was modelled in an RStoich block with a calculator block (Excel based) that estimated the stoichiometric parameters to obtain the reported empirical product distribution [98]. Unconverted H_2 was separated in a Flash and recycled, while liquid HC product was fractionated in a series of RadFrac.

Finally, the kerosene hydrocarbon range streams obtained from the FT synthesis, oligomerisation and wax cracking units were mixed. They entered the isomerisation reactor modelled with an RYield and a calculator block to get the SAF stream with the empirical product distribution [94]. Naphtha, diesel and lubricant fractions obtained from the different fractionated distillations along the system were stored in their respective pools as byproducts from the system.

Concerning the two auxiliary blocks, the light gases were sent to the combined cycled gas turbine unit for energy production. Air was compressed in a 4-stage multiple compressor (MCompr) to 1.8 MPa and used to provide the oxygen needed for the combustion, which was modelled in an RStoic block with a 100 % conversion assumed for all the HC

gaseous compound comprising the feed stream. Electricity was generated in two stages. The high-pressure flue gas operated a gas turbine. The heat produced in the combustion was used to generate high-pressure steam (16.5 MPa) and operated a steam turbine [107].

The ASU model was taken from [108] and adapted to our capacity requirements. High-pressure (6.9 MPa) oxygen was produced using an MComp once separated, while low-pressure (1 MPa) did not require further compression and was sent to the oxidation chamber. The byproduct N_2 stream was compressed and considered a commercial system output.

The comprehensive report of material and energy inflows/outflows delivered by running the described model in Aspen Plus was used as input for the posterior LCA.

2.5. Lifecycle assessment

The goal of the LCA was to evaluate the emission intensity of the investigated SAF production pathway and compare the net lifecycle emissions values (with carbon capture technology incorporated) with the CORSIA benchmark values. To allow comparability with CORSIA, the functional unit was defined as g CO_2e MJ^{-1}.

The system boundary is depicted in Fig. 5, comprising biomass sequestration, biomass supply chain, biomass-to-SAF conversion, fuel transportation, CO_2 capture, kerosene supply chain and combustion in aircraft. Biogenic and fossil CO_2 and GHG released to the atmosphere were also considered. The emissions associated with utilising the captured CO_2 were not considered, and there was not within the scope of this research. An attributional LCA with a well-to-wake perspective was performed [109]. The LCA followed ISO14040/44 guidelines and was performed in SimaPro® 9.1. The lifecycle impact assessment (LCIA) was ILCD 2011 Midpoint + V1.11 to classify and characterise climate change impacts and estimate the resulting net airborne emission of the system while separately considering both biogenic and fossil carbon dynamics [110]. When more than one fuel is produced, an energy-based allocation method, considering the LHV of each fuel, was implemented [52,111]. Data to evaluate the transport and storage of CO_2 was taken from [112]. The calculation of the fuel consumed during aircraft operation was carried out using the model implemented by [113] and considering an Airbus 330–300 as the long-haul plane exemplar [114].

Based on the LCA results, the net carbon balance (B_{TOT}) and the net emissions (NE) are calculated, see Eq. (2) and Eq. (3), respectively. The net CO_2 balance represents the net atmospheric carbon flux of the studied system, i.e., the sum of carbon uptake (sequestered biogenic CO_2 during plant growth) and release (emissions generated along the SAF supply chain). The net emissions account for the difference between the GHG emissions released to the atmosphere and the avoided emissions from using CCS technology to evaluate the impact of the CCS integration.

$$B_{TOT} = -F_{BS} + F_{BSC} + F_{CT} + F_{CCSi} + F_{JA1} + F_{AO} \quad (2)$$

$$NE = F_{BSC} + F_{CT} + F_{JA1} + F_{AO} - F_{CS} \quad (3)$$

where the GHG emissions mass flows, expressed as g CO_2 equivalents per MJ of SAF produced, are as follows: F_{BS} is the carbon fixed in the biomass via biological sequestration, F_{BSC} are the biomass supply chain emissions, F_{CT} are the conversion process emissions, F_{CCSi} are the emissions related to the CCS infrastructure operation, F_{JA1} are the Jet A1 supply chain emissions, F_{AO} are the emissions from fuel burning in aircraft operations and F_{CS} is the carbon stored underground by CCS.

2.6. Sensitivity analysis

Despite being aware using 100 % FT-IPK is not technologically feasible with current jet engines, this could represent the final goal in the defossilisation of international aviation. The FT-SPK production system studied here is not rigid and is subject to change. To investigate the consistency of the net emission score delivered, variations throughout the supply chain were suggested to check the sensitivity of the system's net emissions. Thus, the effect of altering the assumptions set during the modelling for the hydrogen consumption, the catalyst supply chain emissions, the location of biomass pre-treatment (centralised vs decentralised) and the incorporation of aromatics (fossil-based versus bio-based) in the SAF formula was evaluated. Justification and details of each variation are explained in the subsections below.

2.6.1. Hydrogen consumption

The Anderson-Schulz-Flory (ASF) distribution assumes that FT hydrocarbons synthesis is regular [115], i.e. the FT reactor will operate as a polymerisation reactor where only saturated hydrocarbons (paraffins and naphthenes) were obtained. However, experimental data for low-temperature FT (LTFT) reports that the FT product typically comprises 15 %-20 % alkene content and 5 % oxygenated content (mainly alcohol and small proportions of esters and ethers) [92]. Catalyst deactivation decreases its hydrogenating power so that the unsaturated content in the biocrude increases [115]. This would mean hydrogen conversion in the FT reactor is considerably lower, as the unreacted hydrogen will join the FT gaseous product stream, which is not entirely recycled to the reactor. Further hydrogenation in the downstream processing will saturate the

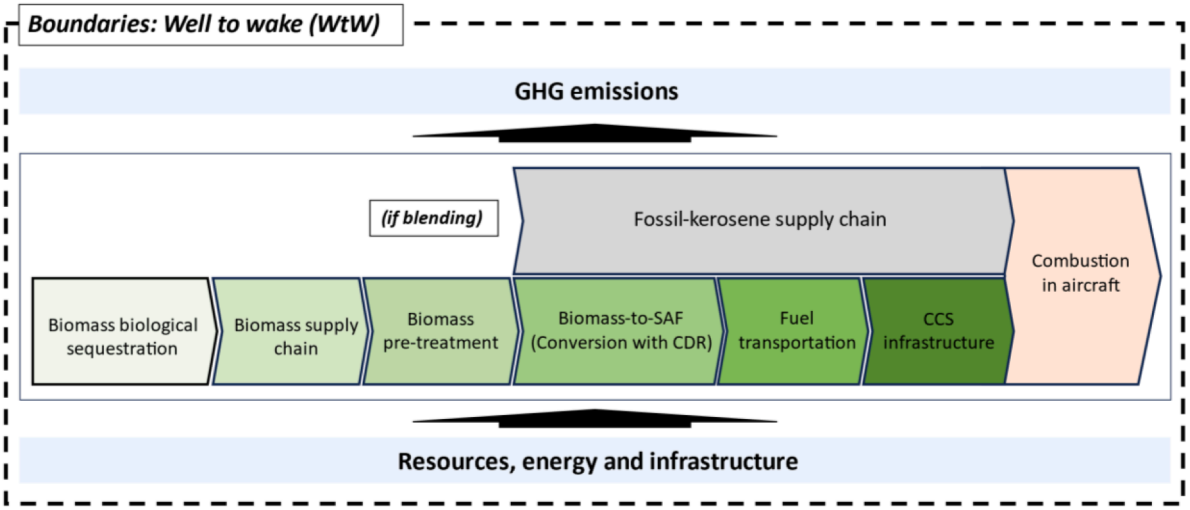

Fig. 5. System boundary for SAF supply chain within this study

double bond and dehydration of oxygenates, leading to a higher hydrogen consumption. Observing the effect of increasing the external hydrogen supply on the net emissions score is important. All the hydrogen externally supplied is assumed to be produced from natural gas reforming (see LCA inventory in the Supplementary material).

2.6.2. Emissions allocated to the catalyst

The full FT-IPK process relies on an extensive amount of catalyst, including the stages of WGS reaction [116,117], FT synthesis [118], oligomerisation [119], wax cracking [120] and isomerisation reactions [97]. LCA studies on full FT-IPK processing rarely include the emissions associated with the catalyst supply chain [50,121]. To understand whether and how the high requirement for catalyst affects the overall emission score has been addressed in the sensitivity analysis. This includes the catalyst/reactant feed ratio at each relevant reaction step and the catalyst flow in the annual process operation. The catalysts' shelf life and regeneration cycles were also considered when regeneration is possible. Attrition limits catalysts shelf life [84], so calculations are based on a catalysts' average lifespan of 5 years [122]. This analysis allows to measure the impact of catalysts' supply chains in the overall emissions results and compare the outcome from this work with previous studies not including this contribution. Considering it or not would provide upper and lower bounds on the environmental impact of this SAF production pathway.

2.6.3. Decentralisation of biomass pre-treatment

In the baseline model, biomass was dried with excess heat from the FT-IPK conversion process at the biomass-to-fuel conversion facility. Alternatively, wood could be pre-treated at the collection point to reduce the moisture content from 50 % to 7 % before transport. Decentralised feedstock pre-treatment reduces the volumetric constraints and increases transportation capacity. Two different energy vectors were assessed for the decentralised drying and torrefaction: electric kiln and natural gas kiln. Specific efficiencies and energy input of the two types of rotary kilns were considered in the study [123]. The environmental impacts were computed according to their respective energy source externally supplied. Transportation was matched with biomass's current volume and weight with similar truck mileage.

2.6.4. Incorporation of aromatics into the SAF formula

Aromatics compounds provide the jet fuel with seal-swell and other needed "fit-for-purpose" (FFP) properties [124]. ASTM regulations require a minimum aromatic content of 8 vol%[125] for SAF to be considered a drop in fuel for commercial aviation. Blending aromatics into the FT-IPK could be an affordable option to match the ASTM requirements for jet fuel (see Section S.5 of Supplementary material). Selecting the appropriate aromatic type, molecular weight, and total concentration could achieve the desired degree of volume swell while also increasing the density of the SAF [126]. The emission impacts of fossil-based and bio-based aromatics under a cradle-to-gate perspective were obtained from the literature. A BTX fraction was assumed as the aromatic additive blended with the FT-IPK. Bio- and fossil-based BTX production were accounted for to measure this blendstock's impact on the SAF's total emissions score. Aromatics produced from biomass reported a net GHG impact of −1.16 kg CO_2e kg BTX^{-1}, obtained as an average value of three scores from past studies [127–129]. The negative value indicates the sequestration of CO_2 during feedstock growth was accounted in the LCA for bio-based aromatics. Conversely, average net emissions of fossil-based aromatics were 4.68 kg CO_2e kg BTX^{-1} [127,128,130]. Upstream supply chain impacts, i.e., transportation to the fuel blending facility, were also considered assuming an average travelling distance of 200 km.

2.7. CORSIA model description and benchmarking

The CORSIA framework provides a Default Lifecycle Emissions Value (LS_f) for the SAF produced from forest residue via the FT pathway [50,121]. Any airline claiming emissions reduction must account for 8.3 g CO_2e per MJ of SAF utilised. Table 3 shows this score was calculated as the median of three different estimations, two of them employing The Greenhouse Gases, Regulated Emission and Energy use in Technology (GREET) model[131] and an additional employing the E3 database [132]. The LS_f was used as a benchmark to compare the outcome presented in this work under a well-to-wake perspective. The system boundary of CORSIA consists of the full supply chain of SAF production and use, including feedstock harvesting, collection and recovery, feedstock processing and extraction, feedstock transportation to processing fuel production facilities, feedstock-to-fuel conversion processes, fuel transportation and distribution. Biogenic carbon was considered climate neutral, so biological sequestration and fuel combustion were not accounted [50].

When employed by both the Massachusetts Institute of Technology (MIT) and the Joint Research Center European Commission (JRC), the GREET model calculated higher total emissions than the E3 database estimations [50]. Feedstock-to-fuel conversion step contribution resulted in zero emissions for the GREET model since GHG emissions credits were accounted for from the process power co-generation, which is assumed to displace an equal amount of US average grid emissions [133]. The E3 model reported higher emissions for feedstock production because of the higher energy demand assumed at the collection. Still, transportation distances were shorter, thus showing a lower impact [50].

3. Results

3.1. Process modelling

The technical performance results of biomass to SAF via FT conversion, including CO_2 capture, are presented in Table 4. Mass and energy balance can be found in the Supplementary material (section S.2). Table 5 shows the material inputs and product outputs for the FT-IPK pathway modelled.

For the described operational scale and process, 145 t kg h^{-1} pine wood was required to generate 185.1 MW of liquid FT hydrocarbon fuels. The biomass-to-liquid fuel efficiency was 51 %, calculated on a dry basis (16.95 MJ kg^{-1}). The total electricity and heat consumption were 33.4 MWe and 140.5 MWth, respectively, mainly due to the energy-intensive pre-treatment processing (74.4 MW) and the multiple distillation stages required to separate the different product fractions. The heat demand, however, could be internally satisfied after performing heat integration to the process due to the highly exothermic nature of the FT synthesis and the heat recovered from the gasifier. Conversely, only 85 % of the power requirements could be co-generated at the CCGT, so an external power supply was needed. The ASU (12.8 MW), the grinding of torrefied wood (6.1 MW) and the captured CO_2 compression (4.5 MW) reported the largest power demand. The pre-combustion carbon capture using Selexol technology allowed to capture 72 % of the CO_2 produced in the process, generating 56.7 t h-1 of CO2 with 99 w % purity. As per the functional unit, 84.7 kg CO_2 MWh^{-1} was captured. The high-pressure conditions of the upstream process enable solvent recovery by adiabatic expansion and reduce the energy required for the Selexol process to capture CO_2. The energy penalty is limited to electricity use for pumping and chilling the solvent, consuming 0.19 MJ per kg CO_2 captured (8 % of the process power demand).

Based on the ASF distribution, results showed that 145 t kg h^{-1} of biomass generated 6,775 kg h^{-1} of FT-IPK. In addition, gasoline (6,386 kg h^{-1}), diesel (1,827 kg h^{-1}) and lubricant (202 kg h^{-1}) were produced as by-products despite the process was designed to maximise SAF production. The fate of the biogenic carbon in the biomass biologically sequestrated from the atmosphere was tracked, performing an atom balance throughout the process. As illustrated in Fig. 6, 44% of the biogenic carbon was captured in the CDR unit and permanently stored

Table 3
LCA results for forest residue FT pathways [g CO_2e MJ^{-1}]. .

Feedstock	Data provider	Model	Feedstock cultivation and collection	Feedstock transportation	Feedstock-to-fuel conversion	Fuel transportation	Total	Midpoint value (LS_f)
Forest residues	MIT	GREET	1.4	3.8	0	0.9	6.1	8.3
	JRC	GREET	2.4	3.8	0	0.9	7.1	
	JRC	E3	3.3	2.9	4	0.3	10.5	

Adapted from [50]

Table 4
Technical performance of the biomass to sustainable aviation fuel (FT-IPK) conversion process.

Parameters	Process modelling results
Biomass input (kg h^{-1})	145,000
Biomass energy content (MW)	351.6
Power consumption (MWe)	33.4
Heat consumption (MWth)	140.5
Internal power production (MWe)	28.8
Internal heat production (MWth)	189.1
Net power requirement (MWe)	4.7
Net heat output (MWth)	48.6 (excess)
Liquid fuels energy production (MW)	185.1
Biomass-to-liquid fuel efficiency (dry basis)	51 %
CO_2 capture rate at CCS unit	95 %
Net CO_2 capture	72 %
CO_2 captured per unit of energy produced (kg CO_2 MWh^{-1})	310.5
Captured CO_2 concentration (mass%)	99.0
Airborne CO_2 emissions per unit of energy produced (kg CO_2e MWh^{-1})	118.0

Table 5
Raw materials and products of the forest residue conversion to sustainable aviation fuel (FT-IPK).

	Mass flow (kg h^{-1})	LHV (MJ kg^{-1})	HC-range
Raw materials			
Biomass input	145,000	16.95	–
Air	190,045	–	–
Water	19,080	–	–
Hydrogen	67	120.1	–
Products			
Iso-paraffinic kerosene (IPK)	6,775	43.8*	$C_8 - C_{16}$
Gasoline	6,386	43.9*	$C_4 - C_{10}$
Diesel	1,827	44.0*	$C_{12} - C_{20}$
Lubricant	202	43.9*	$>C_{20}$
			Purity
Nitrogen	96,975	–	99.1 %

* Calculated based on hydrocarbon blend composition (see Supplementary Material) and an average of the two methods described in [134]. Average LHV for Jet A1 fuel is 43.2 M J kg^{-1}.

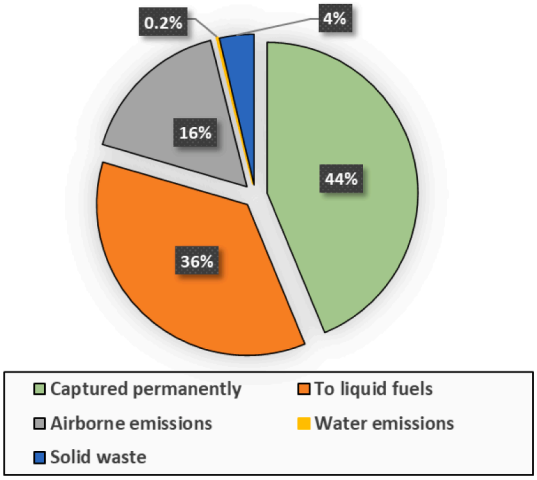

Fig. 6. Fate of the biogenic carbon (biomass)

Table 6
Carbon attribution per stage of the aviation fuel supply chain. Results are shown per MJ of aviation fuel utilised to operate an aircraft.

(g CO_2e MJ^{-1})	Conventional Jet A1 fuel[121]		FT-IPK (100 mass%)		Jet A1 and FT-IPK (50 mass%)	
	Biogenic	*Fossil*	*Biogenic*	*Fossil*	*Biogenic*	*Fossil*
CO_2 biological sequestration	–	–	−128.1	–	−64.5	–
Emissions – Biomass supply chain	–	–	0.1	11.0	–	5.6
Emissions – SAF production process	–	–	15.7	9.9	7.9	5.0
Emissions – CCS Infrastructure	–	–	0.1	0.7	0.1	0.3
Emissions – Aircraft operation	–	72.9	70.7	–	35.6	36.2
Emissions – Jet A1 Cradle to Gate	–	8.9	–	–	–	4.4
CO_2 captured	–	–	56.4	–	28.4	–
Total GHG emissions	81.8		108.1		95.0	
Net GHG balance	81.8		−20.0		30.5	

underground. A 36 % was converted into liquid fuels (including FT-IPK, gasoline, diesel and lubricant), so it will be returned to the atmosphere once burnt. The rest of the biogenic carbon was directly emitted to the environment, with 16 % released back into the atmosphere, 4 % constituting solid wastes (soot sludge and filtered carbon particles), and 0.2 % going into water effluent (dissolved carbon gases).

3.2. Lifecycle assessment

The LCA results report GHG emissions as CO_2 mass equivalents generated per unit of fuel energy (g CO_2e MJ^{-1}) used. Both biogenic and fossil carbon were accounted for to evaluate the effect of incorporating CCS technology in the FT process. The LCA results are presented in Table 6. Three different fuels were investigated and compared: conventional Jet A1 fuel, FT-IPK and the ASTM-certified blend of Jet A1 and FT-IPK (50 mass %). The LCA inventory can be found in section S.4 within the Supplementary information. The GHG emissions contributors have been classified into six main categories: CO_2 uptake during biomass growth, biomass supply chain, biomass-to-SAF conversion process, Jet A1 cradle-to-gate supply chain, CCS infrastructure, and aircraft operation. Since the biomass-to-SAF process also produces three biofuel byproducts, an energy-based allocation method was employed to partition the GHG emissions corresponding to aviation fuel.

The LCA results have shown that from the conventional Jet A1 fuel, cradle-to-gate emissions are 8.9 g CO_2e MJ^{-1}, while 72.9 g CO_2e MJ^{-1} is emitted during fuel combustion at the aircraft [121]. This results in total net emissions of 81.1 g CO_2e MJ^{-1}, all having a fossil origin.

Assuming only FT-IPK is used to operate an aircraft, feedstock requirements sequestered 128.1 g CO_2 MJ^{-1} from the atmosphere during biomass growth. The biomass supply chain typically encompasses land

management, biomass processing and transportation, which accounted for 11.1 g CO_2 per MJ. During biomass conversion, the emissions were 25.6 g CO_2e MJ^{-1}. The emissions associated with the CCS system accounted for 0.8 g CO2e MJ^{-1}, including transporting the CO_2 through pipelines and building and operating the geological storage infrastructure. During aircraft operation, 70.7 g CO_2e per MJ was released. Permanently capturing through CCS 56.4 g of biogenic CO_2 per MJ of aviation fuel used allowed the FT-IPK system to outstrip fossil emissions and remove −20.0 g CO_2e MJ^{-1} from the atmosphere.

The LHV of the produced FT-IPK blendstock (43.8 MJ/kg) was slightly superior to the average reported for Jet A1 fuel (43.2 MJ/kg). Since the LCA functional unit is energy-specific, 1 MJ of 50:50 mass FT-IPK and Jet A1 blend involved 0.504 MJ FT-IPK and 0.496 MJ Jet A1 contributions. Emissions associated with FT-IPK production were approximately, but not exactly, half of the values reported for the previous case. The ASTM-certified blend additionally incorporated the emissions associated with the conventional Jet A1 required (0.023 kg Jet A1/MJ FT-IPK). Jet A1 supply chain contribution was 4.4 g CO_2e MJ^{-1}. Burning the SAF blend during aircraft operation released 71.8 g CO_2e MJ^{-1}. The CCS captured 28.4 g CO_2e MJ^{-1} from the biomass conversion process, which resulted in a total net GHG balance of 30.5 g CO_2e MJ^{-1} from the use of blended Jet A1/FT-IPK.

Table 6 also shows how the two SAF blendstocks' total emissions, including biogenic and fossil carbon, generated superior total GHG emissions than fossil Jet A1 fuel. It is common practice to assume biogenic emissions are climate neutral (e.g. CORSIA framework), so emissions mitigation is sustained on the reduced fossil GHG generated along the supply chain. The suitability of this assumption is questioned in the discussion section.

4. Discussion

In 2023, aviation industry recovered pre-COVID-19 pandemic activity. The UK consumed approximately 14.5 Mt of aviation fuel in 2019, with an 85 % net import rate [135], ranking the UK as the second highest jet fuel consumer after the US [136], and generated 39.6 Mt CO2e [137]. In alignment with the Climate Change Act 2008, the UK has pledged to fulfil 4 % of its aviation fuel demand with SAF by 2025 [137]. This commitment establishes a baseline market size of 0.6 million metric tons of SAF annually in the UK, with anticipated expansion in subsequent years to meet the SAF mandate that seeks to have at least 10 % of SAF (c. 1.2 Mt $year^{-1}$) in the UK aviation fuel mix by 2030 [138]. The UK Carbon Budget Delivery plan was established to annually reduce aviation emissions by 0.029 Mt CO_2e (period 2023–2027), 0.093 Mt CO_2e

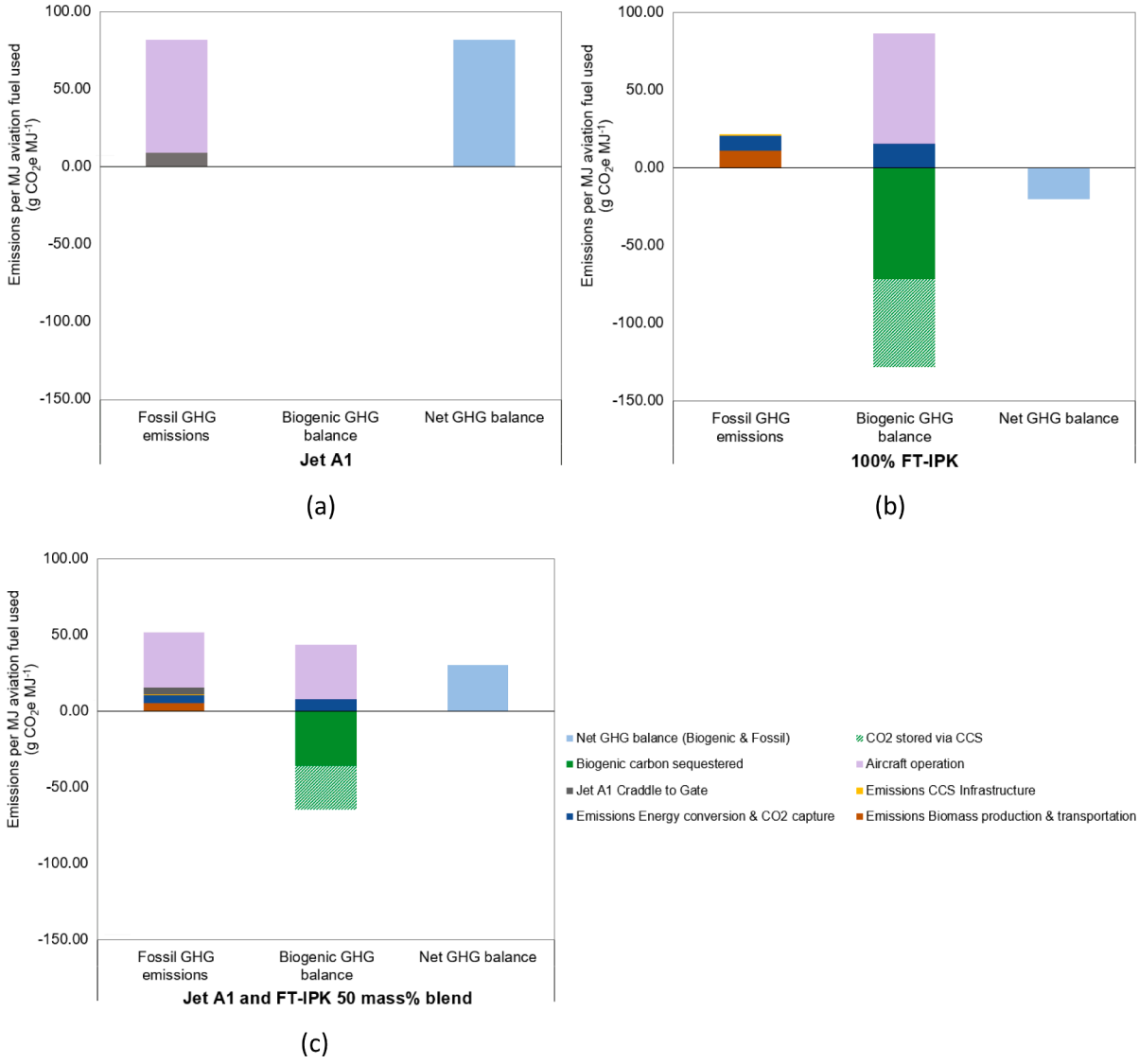

Fig. 7. GHG emissions, CO2 net balance and net emissions from three different aviation fuels: (a) Jet A1 fuel, (b) 100 w % FT-IPK and (c) ASTM blend Jet A1 with 50 w % FT-IPK

(period 2028–2032) and 0.2 Mt CO_2e (period 2033–2037) [139].

The performance of process modelling for the analyzed SAF production pathway allowed to estimate the biomass to SAF conversion process yield. Assuming the upper bound for the availability of domestic sustainable forestry residues, i.e., 2.0 Mt p.a., and no competition for resources, two facilities of the investigated scale (6.8 t SAF h^{-1}) could be operated with a capacity factor of 80 %. 0.1 Mt of FT-IPK could be produced, replacing 0.7 % of the UK's aviation fuel demand.

The LCA calculated the GHG emissions generated from each investigated aviation fuel blendstock. Fig. 7 depicts the breakdown of the carbon emissions, differentiating biogenic and fossil based GHG contributions, for the three types of aviation fuel evaluated in this work.

Using Jet A1 fuel to operate an aircraft result in a positive carbon flux from a carbon reservoir to the atmosphere that has been stored for millions of years. Emissions associated with extraction, processing, transportation and storage are aggregated to score a final positive carbon balance (81.1 g CO_2e MJ^{-1}) within the system boundaries described. Including a biogenic fraction on the jet fuel implies that part of the carbon emitted to the atmosphere has been previously sequestered from it in a relatively short time during biomass growth. This is the basis for assuming biogenic emissions are climate neutral. Thus, an aircraft fuelled with FT-IPK could cut down fossil GHG emissions by 74 % concerning Jet A1 score (see Fig. 7a and 7b). Since commercial jet engines are yet unable to operate only with SAF, using the ASTM-certified Jet A1 and FT-IPK blend (Fig. 7c) reduced fossil emissions by 37 %. Adapting jet engines to run on 100 % FT-IPK could lead to a substantial reduction in fossil carbon emissions comparable to synthetic e-fuels pathways, which reported lifecycle emissions savings that range between 50 and 90 %, while the energy intensity is significantly lower (0.01 MJ/MJ liquid fuel), measuring two orders of magnitude below than those alternatives [40,53,55].

Presuming biogenic emissions are equivalent to CO_2 fixation overlooks the formation of other biogenic-origin GHG with different global warming potential (e.g. methane) or further non-CO_2 climate impacts. However, in this case study, gaseous streams reaching the atmosphere were flue gases from combustion, and well-to-wake biogenic methane flow resulted negligible ($<2 \times 10^{-3}$ g CO_2e MJ^{-1} SAF). The study of non-CO_2 climate impacts is beyond the scope of this study. Still, assessments around quantification are important for these phenomena and are discussed in the literature [140–142].

Understanding the potential of integrated CCS technology in the FT-IPK production process can only be acknowledged when considering biogenic carbon dynamics. Similarly to bioenergy with carbon capture and storage, the carbon removal potential is achieved from the carbon biologically sequestered from the biomass, and the ratio of that carbon is permanently fixed via CCS [52]. When that fraction of biogenic carbon stored is superior to the fossil-carbon emitted, a net-negative flux of atmospheric carbon can be created. Fig. 7b shows a net negative GHG balance since the biogenic carbon sequestered (central column) is larger than the positive fossil GHG emissions (left column). The carbon sequestered in the ASTM-blend system (Fig. 7c) cannot entirely offset the fossil emissions due to the lesser biomass requirements to produce one unit of aviation fuel and the fossil carbon emitted by the Jet A1 fraction. The net GHG balance is still positive but inferior to the total fossil-GHG emissions measured in the LCA.

When using the proposed pathway sourced with the domestic forest residue available, accounting for the results from this study and considering biogenic emissions as climate neutral following the mandate, fossil GHG emissions can be reduced by 0.24 Mt CO_2e p.a. Considering both fossil and biogenic carbon dynamics, the effective mitigation on aviation GHG emissions was 0.41 Mt CO_2e p.a. The values reported are equivalent regardless, assuming the FT-IPK is blended with Jet A1 to meet ASTM standards or used alone to fuel the aircraft. The factor limiting emissions mitigation was the amount of biomass dedicated to producing the SAF blendstock. It can be inferred that dedicating the available UK forest and waste wood residues to produce SAF via Fischer-Tropsch could satisfy the emission reduction goal for international aviation in the UK for 2037, but only when CCS technology is integrated. However, the share of SAF targeted to cover UK aviation fuel demand cannot be reached only by this route, and other SAF production pathways must be parallelly implemented.

These reductions can be achieved by deploying commercially proven technologies. However, these are modelling values, and the sensitivity analyses provided more detail on the environmental performance and possible variations based on operational and performance characteristics. Moreover, with the implementation of CORSIA and the increasing need to decarbonise the aviation sector, the results of this study are set into the context of the CORSIA framework.

4.1. Sensitivity analysis on emissions reductions from SAF utilisation

Table 7 summarises the results of the sensitivity analyses of FT-IPK 100 (w%) compared to fossil-based Jet A1 fuel. It presents the net emissions (g CO_2e MJ^{-1}) of the FT-IPK (w%) and the emission reduction compared to Jet A1 use (%), e.g. net fossil carbon emissions of 21.6 g CO_2e MJ^{-1} for FT-IPK (100 w%) mean an emission reduction of 74 % compared to Jet A1.

4.1.1. Hydrogen consumption

Sensitivity A considered an additional H_2 consumption to hydrogenate the FT products with higher content of unsaturates due to Anderson-Shulz-Flory (ASF) model inaccuracies and catalyst deactivation. The supplementary hydrogen consumption was calculated using experimental data from the hydrogenation of alkenes with one and two degrees of unsaturation, alcohols [143], esters [144] and ethers [145]. The highest unsaturates content in the FT product was assumed, i.e., 20 % of alkenes (with a 3:1 ratio of components with 1 and 2 unsaturations, respectively) and 5 % of oxygenates (with a 90 % alcohol, 9 % ester and 1 % acid distribution) [146]. As previously stated, hydrogen produced from natural gas reforming was the external sourcing selected to feed the process. Hydrogen consumption resulted in 236 % higher than in the benchmark case study. Compared to the baseline results, the net GHG emissions score for the SAF resulted in no significant additional emissions generated from the increased hydrogen supply (see Table 7). The possibility of underestimating hydrogen requirements from assuming higher hydrogenation, hydrocracking and isomerisation efficiencies still exists. However, the hydrogen consumption assumed in this work

Table 7
Sensitivity analysis over net CO_2 balance, net emissions, and emission reduction for Jet A1 use, FT-IPK supply and utilisation.

	FT-IPK (100 w%) GHG emissions (g CO_2e MJ^{-1})		Net GHG balance (g CO_2e MJ^{-1})	Fossil emissions reduction to Jet A1 (%)
	Fossil	*Biogenic*		
Baseline value	21.6	86.5	−20.0	74
Sensitivity A: Higher H_2 requirements	21.7	86.5	−19.9	74
Sensitivity B: No catalysts supply chain impact	16.8	86.5	−24.8	80
Sensitivity C1: Decentralised torrefaction (electric kiln)	31.0	86.5	11.9	62
Sensitivity C2: Decentralised torrefaction (natural gas kiln)	42.8	82.8	20.0	48
Sensitivity D1: Aromatic addition (fossil-based)	33.1	84.6	5.3	59
Sensitivity D2: Aromatic addition (bio-based)	19.1	84.6	−11.8	77

resulted superior to previous studies evaluating similar FT processes with product upgrading [98]. The sensitivity study outcome indicates that the energy source used to produce hydrogen is irrelevant when used in the present process, so renewable hydrogen should be employed for other activities with higher influence on the environmental impact.

4.1.2. Emissions allocated to the catalyst

Despite being a crucial element in the FT-IPK emissions assessment, many studies overlook the significance of catalyst supply chains. This study revealed that 22 % of the biomass-to-jet fuel process GHG emissions (equivalent to 4.8 g CO_2e MJ^{-1}) were associated with the metal catalysts supply chain, having all a fossil origin. This finding indicates that the contribution of the catalyst supply chain towards FT-IPK emissions is significant. Excluding its impact from calculations can lead to mistakenly accounting for an emission reduction of up to 80 % instead of 74 %, as per our baseline value findings. Moreover, acute catalyst deactivation leading to reduced shelf life concerning the estimated one or the impossibility of implementing a catalyst regeneration process would greatly increase catalyst consumption rates and substantially aggravate the SAF's emission impact.

4.1.3. Decentralisation of biomass pre-treatment

Sensitivity C assessed the emission implications of drying biomass at the collection point and before transport using an electric and a natural gas kiln. Direct implications mainly include the need for an external energy source to power the pre-treatment kiln. Milling was still considered to be performed at the conversion facility. The excess heat from the SAF process, originally used for onsite biomass torrefaction, was utilised in the steam turbine for electricity production. The extra power generation allowed the process to match the internal electricity demand. At the same time, a 4 MWe surplus enters the national grid. Since electricity is an additional energy byproduct of the process, energy allocation factors in the LCA were recalculated (see Supplementary material). Carbon credits from displacing UK grid electricity were considered [147].

Results compiled in Table 7 show that decentralised biomass pre-treatment negatively affects the environmental impact of the SAF, in line with results from previous research evaluating decentralised SAF production [148]. Emission savings from reducing transportation and generating low-carbon electricity could not compensate for the carbon footprint of the external energy supply required for biomass pretreatment. This outcome holds under the assumptions taken for biomass freight distance (100 km). A much larger travelling distance for biomass could close the gap. Indirect heated rotary kilns fuelled with natural gas resulted in higher fossil emissions when compared to electric kilns due to differences in the energy efficiency reported for each equipment, i.e. 40 % and 95 % of the energy input, respectively. Since both decentralised scenarios worsened the emission score for the SAF, the benefit from recycling internal energy waste streams increased the system's overall efficiency. However, if the electricity were fully decarbonised, the emission profile of the electrified decentralised option would result in 13.1 g CO_2e MJ^{-1} FT-IPK, thus representing the scenario with the largest reduction in fossil emissions (84 %).

4.1.4. Incorporation of aromatics into the SAF formula

Sensitivity D quantified the variations on the impact of the SAF's net GHG emissions from adding 10 vol% of aromatics to meet ASTM requirements for aviation fuel to operate jet engines. 3 g BTX per MJ of FT-IPK were needed to reach that threshold. Fossil-based and bio-based aromatics LCA data encompassing the additive's supply chain were considered. Blending the SAF with a fossil-based aromatics additive penalised the carbon footprint of the produced fuel by adding 14.2 g CO_2e MJ^{-1}. Net fossil GHG emissions increased a 35 % concerning the FT-IPK, which prevented the system from removing CO_2 from the atmosphere (the net GHG balance turned positive).

Conversely, using bio-based aromatics reduced 13 % of the net fossil GHG emissions of the SAF. Despite bio-based aromatics feedstock also sequestered CO_2 before converting them into BTX products, the biomass-to-BTX yield of the process seemed more efficient and less mass of feedstock is required to generate 1 MJ of FT-IPK and additive blend. The net GHG balance of the system was negative (-11.8 g CO_2e MJ^{-1}). Still, it removed less atmospheric carbon than using solely FT-IPK (-20.0 g CO_2e MJ^{-1}).

The minimum density threshold set by the ASTM, i.e., 775 kg/m^3, could not still be achieved. The resulting blend (696.7 kg/m^3) would require a thickener additive to operate commercial jet engines.

4.1.5. Summary of the sensitivity analysis

Fig. 8 represents the sensitivity analysis results of the three parameters representing the emissions reduction when substituting fossil jet A1 aviation fuel with FT-IPK. Net GHG balance reported the wider and less concentrated spread, showing the highest sensitivity towards process and supply chain modelling assumptions. Fossil GHG emissions factor showed the narrower range located around an average of 27 g CO_2 per MJ of FT-SPK utilised.

4.2. Comparison between CORSIA score and modelling results

Fig. 9 compares the CORSIA score obtained using the GREET and E3 models [50,121,131,132] and the LCA results of the presented study. The graph illustrates the emission scores for each supply chain category (feedstock cultivation and collection, feedstock transportation, feedstock conversion and fuel transportation) and the total emission score of the assessed cradle-to-gate supply chain.

At feedstock cultivation and collection, the GREET model uses forest residues of poor quality and unsuitable for the timber markets, such as branches, tops of stems, diseased wood and deadwood, considered waste or by-products [149]. By comparison, the feedstock cultivation and collection emissions of the E3 model as it assumes a higher energy demand for feedstock collection than GREET (0.26 CO_2e MJ kg^{-1}, compared to 0.14 CO_2e MJ kg^{-1}) [50]. In the presented study, emissions at feedstock cultivation and collection point were derived from forest management, harvesting, chipping and handling the biomass amounting to 6.7 g CO_2e MJ^{-1}. As for GREET and E3, this study considers the use of residual and low-quality wood and emissions were allocated between the different forest products. Furthermore, GREET and E3 both assume co-firing (coal + biomass), which explains a lower LCA score.

In GREET, the feedstock transportation distance of 144.8 km using a heavy-duty truck. The E3 database has a shorter distance of 50 miles

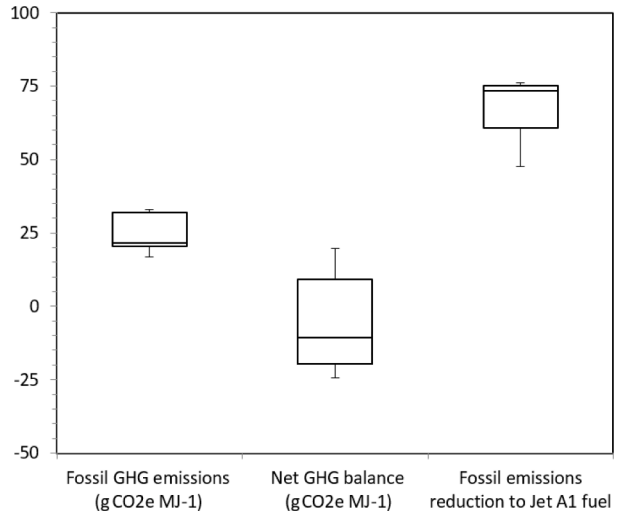

Fig.8. Sensitivity analysis over fossil GHG emissions, system's net GHG balance, and Jet A1 fossil emissions reduction percentage from using FT-IPK.

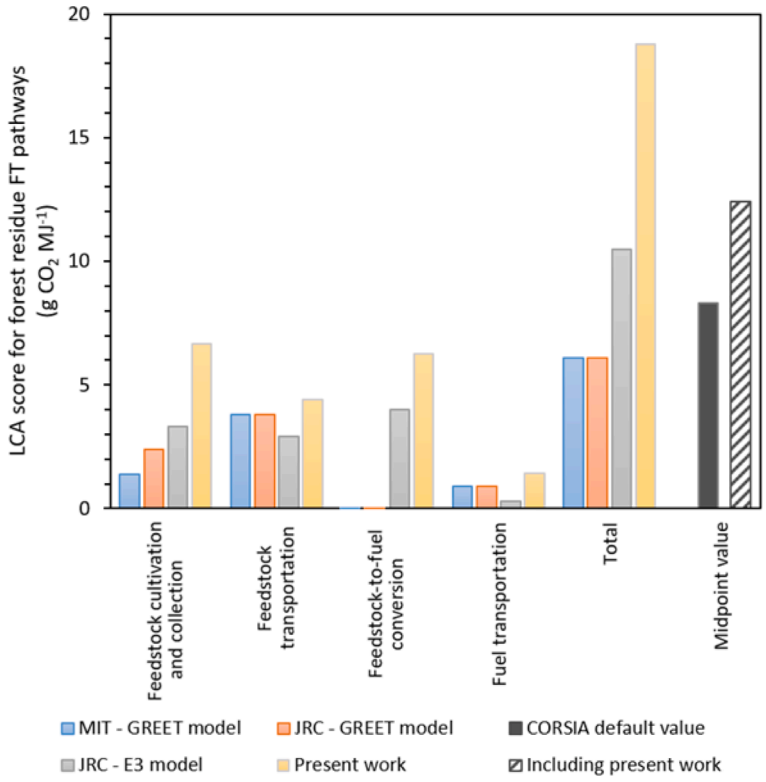

Fig. 9. LCA score for forest residue conversion to SAF via FT synthesis

[124]. The distance assumption used in the study was 200 km in a 15 t lorry. This led to slight variations in the results comparing the two CORSIA models and the here presented research.

At the feedstock-to-fuel conversion point, the GREET and E3 models assume emissions of 0.03 and 4 g CO_2e MJ^{-1}, respectively. Both models state that only isomerisation was considered during syngas upgrading; therefore, the emission scores are significantly lower than in the presented study. Our LCA resulted in 6.3 g CO_2e MJ^{-1}, mainly from biomass torrefaction. The high demand for metal catalyst usage was also considered, as described above. As a result, the emissions from catalyst production were 22 %, i.e., 4.8 g CO_2e MJ^{-1}. Thus, higher emission scores in this study resulted from assessing the whole supply chain and process, including upgrading the FT products (oligomerisation, wax hydrocracking and isomerisation). This study's FT conversion efficiency of 51 % was similar to the GREET and E3 models, with 50 and 44 %, respectively.

As for feedstock transportation, the assumptions on fuel transportation varied between Greet, E3 and the presented study. GREET assumed a distance of 1,288 km, 837 km and 644 km via rail, barge and pipeline, respectively. E3 database assumed a distance of 250 km via rail travelling.

The LCA results of this study were compared with the CORSIA scores, showing that the total LCA score was nearly four times higher than the CORSIA default lifecycle value. Feedstock cultivation and collection and feedstock-to-fuel conversion had the highest LCA results. The biomass-to-FT-IPK conversion included the catalyst lifecycle, one of the main contributing factors to a high LCA score. The CORSIA scores were collected using the GREET and E3 models. However, this was challenging as there was insufficient information and uncertainties to replicate. Furthermore, it is important to remark that CORSIA scores do not indicate biomass pre-treatment, a highly energy-intensive process necessary to greatly reduce moisture content and particle size of biomass, as a key supply chain stage with high emissions contribution. When the GREET model assumes that the feedstock-to-fuel conversion contribution is negligible, since the substantial power cogeneration within the process displaces emissions from the US grid mix, it can be argued that there is still an energy surplus available to internally satisfy the energy demands of biomass pre-treatment. This assertion is supported by the findings of the process model developed in this study, which indicated that biomass pre-treatment consumed 53 % of the heat and 18 % of the power needed to produce the SAF. The LCA carried out in this work certainly include that stage on the supply chain, which can be the cause from the superior emissions score obtained when compared to CORSIA value.

To effectively reach the objectives of CORSIA scheme, it would be beneficial to have accessible and transparent case studies providing a comprehensive understanding of the emissions generated by the SAF's whole value chain. These case studies can help to verify the claimed emissions reductions resulting from the utilization of that specific SAF. Consequently, it would be advisable to establish a more precise default LCA value, or a set of scores that correspond to various process configurations, for a particular CORSIA-eligible fuel pathway.

5. Limitations of this study

Pinewood was the only biomass considered for SAF production in this study. However, biomass-to-SAF conversion should not be limited to only one feedstock, as biomass is a finite resource and only biomass residues should be considered for biofuel production. Sustainable biomass waste streams, i.e., agricultural waste, could be considered and incorporated for SAF production.

BECCS was incorporated with the SAF production in the process simulation and LCA to realise net-zero targets. With the optimistic process simulation results, BECCS can achieve a net CO_2 capture of 72 %. Future work should include BECCS but not be limited to SAF production to meet net-zero targets. However, more BECCS technologies should be implemented, and further work should be investigated to realise BECCS.

We employed the measures of biogenic CO_2 in the biomass as given by SimaPro, however, those values do not match the carbon atom balance performed in the process modelling. The mass balance indicated

the CO_2 fixed by biomass was 54 % higher than the numbers used in the LCA, so that the net GHG carbon balance would be more negative than the numbers presented here. However, it was preferable to take a conservative perspective and utilise the restricted atmospheric CDR flux.

6. Conclusions

Sustainable aviation fuel from biomass holds great potential for reducing greenhouse gas emissions in the aviation sector. Bio jet fuels offer advantages in terms of ease and speed of deployment as they can reuse the existing technologies and infrastructures and their ability to use equipment with little or no modification. Additionally, SAF blends meet international standards making their deployment internationally promising. While electrification, hydrogen and electric fuel are several alternatives to conventional jet fuel, they do not offer the short and medium-term solutions for the actions we need to take now.

The use of bio jet fuels, such as those produced through the Fischer-Tropsch pathway, has gained momentum. The present research has shown that FT-SPK, combined with carbon capture and storage, can reduce over 74 % fossil GHG emissions when compared to fossil fuel counterparts. The emission savings of this route are similar to those achieved through synthetic e-fuel pathways, but it involves significantly lower energy intensity and can create a net-negative carbon flow from the atmosphere to an underground storage. This highlights the potential of sustainable bio jet fuels to reduce carbon emissions and support net-zero strategies when combined with carbon capture technologies. However, to accurately measure the benefits from SAF replacing conventional jet fuels and the carbon removal capabilities from CCS integration, biogenic and fossil carbon dynamics must be accounted on the LCA.

A mix of low-carbon fuels and solutions, including bio jet fuels, will be required to decarbonise the aviation sector. This study showed that dedicating the whole national waste wood resources for SAF production would result insufficient to meet the targeted SAF share and emission reduction goal for 2050. Different technologies and low-carbon fuel pathways will need to co-evolve, and policy measures and regulatory frameworks will influence how this development will look to some extent. However, policies must also be flexible to respond to changes that support a fast, affordable and resilient supply of low-carbon fuels in line with net-zero targets and keep transport and infrastructure functional.

CRediT authorship contribution statement

Alberto Almena: Writing – review & editing, Writing – original draft, Validation, Methodology, Investigation, Formal analysis, Data curation, Conceptualization. **Regina Siu:** Visualization. **Katie Chong:** Conceptualization. **Patricia Thornley:** Validation, Supervision, Funding acquisition, Formal analysis, Conceptualization. **Mirjam Röder:** Writing – review & editing, Supervision, Methodology.

Declaration of competing interest

The authors declare that they have no known competing financial interests or personal relationships that could have appeared to influence the work reported in this paper.

Data availability

No data was used for the research described in the article.

Acknowledgement

This work was conducted as part of the NewJet Network+, supported by the Engineering and Physical Sciences Research Council (EPSRC) (Grant number: EP/S032118/1), the EPSRC/BBSRC Supergen Bioenergy Hub (Grant number: EP/S000771/1); and the European Union's Horizon 2020 research and innovation programme under the Marie Skłodowska-Curie grant agreement No. 101034371.

Appendix A. Supplementary data

Supplementary data to this article can be found online at https://doi.org/10.1016/j.enconman.2024.118186.

References

[1] ICAO. The World of Air Transport in 2019. 2021.
[2] ICAO. Economic Impacts of COVID-19 on Civil. Aviation 2021.
[3] CCC. Progress in reducing emissions - 2021 Report to Parliament. 2021.
[4] Grewe V, Gangoli Rao A, Grönstedt T, Xisto C, Linke F, Melkert J, et al. Evaluating the climate impact of aviation emission scenarios towards the Paris agreement including COVID-19 effects. Nat Commun 2021;12:3841. https://doi.org/10.1038/s41467-021-24091-y.
[5] Emadi A. Transportation 2.0. IEEE Power Energ. Mag. 2011;9:18–29. https://doi.org/10.1109/MPE.2011.941320.
[6] USDoT Two Decades of Change in Transportation Reflections from Transportation Statistics Annual Reports 1994–2014. 2015.
[7] ATAG. Facts & Figures 2020. https://www.atag.org/component/factfigures/?Itemid (accessed October 12, 2020).
[8] DfT. Jet Zero Consultation. 2021.
[9] EEA Greenhouse gas -. Data Viewer 2020.
[10] Welfle A, Thornley P, Röder M. A review of the role of bioenergy modelling in renewable energy research & policy development. Biomass Bioenergy 2020;136:105542.
[11] Masson-Delmotte V, Zhai P, Pörtner H-O, Roberts D, Skea J, Shukla PR. Global Warming of 1.5 C: IPCC special report on impacts of global warming of 1.5 C above pre-industrial levels in context of strengthening response to climate change. sustainable development, and efforts to eradicate poverty. Cambridge University Press; 2022.
[12] IATA. IATA Annual Review 2015. 2016.
[13] Burgueño-Salas E. Global CO2 emissions from commercial aviation 2004-2022. 2022.
[14] ICAO. Environmental Report Chapter Six - Climate Change Mitigation CORSIA 2019.
[15] Kozuba J, Ojciec M. Overview of historical and future trends of commercial aircraft fuel efficiency. Acta Avionica Journal 2019:12–7.
[16] Coder JG, Somers DM. Design of a slotted, natural-laminar-flow airfoil for commercial transport applications. Aerosp Sci Technol 2020;106:106217. https://doi.org/10.1016/j.ast.2020.106217.
[17] Yang Y, Bai J, Li L, Yang T, Wang H, Ma S, et al. An inverse design method with aerodynamic design optimization for wing glove with hybrid laminar flow control. Aerosp Sci Technol 2019;95:105493. https://doi.org/10.1016/j.ast.2019.105493.
[18] Magrini A, Benini E, Yao H-D, Postma J, Sheaf C. A review of installation effects of ultra-high bypass ratio engines. Prog. Aerosp. Sci. 2020;119:100680. https://doi.org/10.1016/j.paerosci.2020.100680.
[19] Advance and Ultra Fan engines 2021. 2021..
[20] Cheaito H, Allard B, Clerc G. Proof of concept of 35 kW electrical taxiing system in more electrical aircraft for energy saving. Int. J. Electr. Power Energy Syst. 2021;130:106882. https://doi.org/10.1016/j.ijepes.2021.106882.
[21] Wileman AJ, Aslam S, Perinpanayagam S. A road map for reliable power electronics for more electric aircraft. Prog. Aerosp. Sci. 2021;127:100739. https://doi.org/10.1016/j.paerosci.2021.100739.
[22] IATA. Aircraft Technology Roadmap to 2050. 2019.
[23] Ma Y, Elham A. Twin-fuselage configuration for improving fuel efficiency of passenger aircraft. Aerosp Sci Technol 2021;118:107000. https://doi.org/10.1016/j.ast.2021.107000.
[24] J. Fu Z. Shi Z. Gong Lowenberg mh, wu d, pan l. Virtual flight test techniques to predict a blended-wing-body aircraft in-flight departure characteristics Chin. J. Aeronaut. 35 2022 215 225 10.1016/j.cja.2021.01.006.
[25] Kumari S, Dinbandhu AK. Study of machinability aspects of shape memory alloys: a critical review. Mater Today Proc 2021;44:1336–43. https://doi.org/10.1016/j.matpr.2020.11.390.
[26] Abdellatief TMM, Ershov MA, Kapustin VM, Ali Abdelkareem M, Kamil M, Olabi AG. Recent trends for introducing promising fuel components to enhance the anti-knock quality of gasoline: a systematic review. Fuel 2021;291:120112. https://doi.org/10.1016/j.fuel.2020.120112.
[27] Ershov MA, Klimov NA, Burov NO, Abdellatief TMM, Kapustin VM. Creation a novel promising technique for producing an unleaded aviation gasoline 100UL. Fuel 2021;284:118928. https://doi.org/10.1016/j.fuel.2020.118928.
[28] Zamponi R, Chiariotti P, Battista G, Schram C, Castellini P. 3D Generalized Inverse Beamforming in wind tunnel aeroacoustic testing: application to a Counter Rotating Open Rotor aircraft model. Appl. Acoust. 2020;163:107229.
[29] Liu F. Research on Evaluation of Operational Efficiency of Civil Aviation Flight. 2018 International Conference on Transportation & Logistics, Information & Communication, Smart City (TLICSC 2018), Atlantis Press; 2018, p. 504–8.
[30] Hileman JI, Stratton RW. Alternative jet fuel feasibility Transp Policy (Oxf) 2014;34:52–62. https://doi.org/10.1016/j.tranpol.2014.02.018.

[31] Epstein AH, O'Flarity SM. Considerations for Reducing Aviation's CO2 with Aircraft Electric Propulsion. J Propuls Power 2019;35:572–82. https://doi.org/10.2514/1.B37015.
[32] Wei H, Liu W, Chen X, Yang Q, Li J, Chen H. Renewable bio-jet fuel production for aviation: a review. Fuel 2019;254:115599. https://doi.org/10.1016/j.fuel.2019.06.007.
[33] The Royal Society. Sustainable synthetic carbon based fuels for transport: Policy Briefing. 2019.
[34] Brelje BJ, Martins JRRA. Electric, hybrid, and turboelectric fixed-wing aircraft: a review of concepts, models, and design approaches. Prog. Aerosp. Sci. 2019;104:1–19. https://doi.org/10.1016/j.paerosci.2018.06.004.
[35] Nicolay S, Karpuk S, Liu Y, Elham A. Conceptual design and optimization of a general aviation aircraft with fuel cells and hydrogen. Int J Hydrogen Energy 2021;46:32676–94. https://doi.org/10.1016/j.ijhydene.2021.07.127.
[36] Bauen A, Bitossi N, German L, Harris A, Leow K. Sustainable Aviation Fuels: status, challenges and prospects of drop-in liquid fuels, hydrogen and electrification in aviation. Johnson Matthey Technol. Rev. 2020;64:263–78.
[37] Rondinelli S, Gardi A, Kapoor R, Sabatini R. Benefits and challenges of liquid hydrogen fuels in commercial aviation. International Journal of Sustainable Aviation 2017;3:200–16. https://doi.org/10.1504/IJSA.2017.086845.
[38] Doliente SS, Narayan A, Tapia JFD, Samsatli NJ, Zhao Y, Samsatli S. Bio-aviation fuel: a comprehensive review and analysis of the supply chain components. Front Energy Res 2020;8:110.
[39] Daggett D, Hendricks R, Walther R. Alternative fuels and their potential impact on aviation. 25th Congress of the International Council of the Aeronautical Sciences (ICAS 2006), 2006.
[40] Rojas-Michaga MF, Michailos S, Cardozo E, Akram M, Hughes KJ, Ingham D, et al. Sustainable aviation fuel (SAF) production through power-to-liquid (PtL): a combined techno-economic and life cycle assessment. Energy Convers Manag 2023;292:117427. https://doi.org/10.1016/j.enconman.2023.117427.
[41] Ershov MA, Savelenko VD, Burov NO, Makhova UA, Mukhina DY, Aleksanyan DR, et al. An incorporating innovation and new interactive technology into obtaining sustainable aviation fuels. Energy 2023;280:128156. https://doi.org/10.1016/j.energy.2023.128156.
[42] Burov NO, Savelenko VD, Ershov MA, Vikhritskaya AO, Tikhomirova EO, Klimov NA, et al. Knowledge contribution from science to technology in the conceptualization model to produce sustainable aviation fuels from lignocellulosic biomass. Renew Energy 2023;215:118898. https://doi.org/10.1016/j.renene.2023.06.019.
[43] Mustafa A, Faisal S, Ahmed IA, Munir M, Cipolatti EP, Manoel EA, et al. Has the time finally come for green oleochemicals and biodiesel production using large-scale enzyme technologies? Current status and new developments. Biotechnol Adv 2023;69:108275. https://doi.org/10.1016/j.biotechadv.2023.108275.
[44] Sustainable Aviation. Sustainable aviation fuels road-map: Fueling the future of UK aviation. 2020.
[45] The Royal Society. Net zero aviation fuels: resource requirements and environmental impacts. 2023.
[46] Statista. Fuel costs of airlines worldwide from 2011 to 2021, with a forecast until 2023, as percentage of expenditure 2023. https://www.statista.com/statistics/591285/aviation-industry-fuel-cost/ (accessed March 5, 2023).
[47] L. Martinez-Valencia S. Peterson K. Brandt A.B. King M. Garcia-Perez M. Wolcott Impact of services on the supply chain configuration of sustainable aviation fuel: the case of CO2e emission reductions in the U.S J Clean Prod 2023;404:136934. 10.1016/j.jclepro.2023.136934.
[48] European Commission. EU Emissions Trading System (EU ETS). 2015.
[49] CCC. The Sixth Carbon Budget: The UK's path to Net Zero. 2020.
[50] ICAO. CORSIA Supporting Document. COSIA Eligible Fuels - Life Cycle Assessment Methodology. 2019.
[51] Maertens S, Grimme W, Scheelhaase J, Jung M. Options to Continue the EU ETS for Aviation in a CORSIA-World. Sustainability 2019;11:5703.
[52] Almena A, Thornley P, Chong K, Röder M. Carbon dioxide removal potential from decentralised bioenergy with carbon capture and storage (BECCS) and the relevance of operational choices. Biomass Bioenergy 2022;159:106406.
[53] Liu CM, Sandhu NK, McCoy ST, Bergerson JA. A life cycle assessment of greenhouse gas emissions from direct air capture and Fischer-Tropsch fuel production. Sustain Energy Fuels 2020;4:3129–42. https://doi.org/10.1039/C9SE00479C.
[54] Seber G, Escobar N, Valin H, Malina R. Uncertainty in life cycle greenhouse gas emissions of sustainable aviation fuels from vegetable oils. Renew. Sustain. Energy Rev. 2022;170:112945. https://doi.org/10.1016/j.rser.2022.112945.
[55] Peacock J, Cooper R, Waller N, Richardson G. Decarbonising aviation at scale through synthesis of sustainable e-fuel: a techno-economic assessment. Int J Hydrogen Energy 2024;50:869–90. https://doi.org/10.1016/j.ijhydene.2023.09.094.
[56] Saynor B, Bauen A, Leach M. The potential for renewable energy sources in aviation. Imperial College Centre for Energy Policy and Technology: Imperial College, London; 2003. p. 68.
[57] O'Malley J, Pavlenko N, Searle S. Estimating sustainable aviation fuel feedstock availability to meet growing European Union demand. Berlin, Germany: International Council on Clean Transportation; 2021.
[58] Bates J. Biomass Feedstock Availability. Final Report Hg v Ricardo Energy & Environment UK Department for Business. Energy and Industrial Strategy Ricardo/ED662421043/Issue 2017.
[59] Maxwell S. Forestry Statistics 2022. Chapter 1: Woodland Area & Planting. 2022.
[60] Kc R, Babu I, Alatalo S, Föhr J, Ranta T, Tiihonen I. Hydrothermal carbonization of deciduous biomass (Alnus incana) and pelletization prospects. J Sustain Bioenergy Syst 2017;7:138.
[61] Emenike O, Michailos S, Finney KN, Hughes KJ, Ingham D, Pourkashanian M. Initial techno-economic screening of BECCS technologies in power generation for a range of biomass feedstock. Sustainable Energy Technol. Assess. 2020;40:100743.
[62] Yan W, Acharjee TC, Coronella CJ, Vasquez VR. Thermal pretreatment of lignocellulosic biomass. Environmental Progress & Sustainable Energy: An Official Publication of the American Institute of Chemical Engineers 2009;28:435–40.
[63] Tumuluru JS. Effect of deep drying and torrefaction temperature on proximate, ultimate composition, and heating value of 2-mm lodgepole pine (Pinus contorta) grind. Bioengineering 2016;3:16.
[64] Kozakiewicz P, Tymendorf Ł, Trzciński G. Importance of the moisture content of large-sized Scots pine (Pinus sylvestris L.) roundwood in its road transport. Forests 2021;12:879.
[65] Wang T, Stiegel GJ. Integrated gasification combined cycle (IGCC) technologies. Woodhead Publishing; 2016.
[66] Bermudez JM, Fidalgo B. Production of bio-syngas and bio-hydrogen via gasification. Handbook of Biofuels Production 2016:431–94.
[67] Gopalakrishnan B, Mardikar Y, Gupta D, Jalali SM, Chaudhari S. Establishing baseline electrical energy consumption in wood processing sawmills for lean energy initiatives: a model based on energy analysis and diagnostics. Energy Eng. 2012;109:40–80.
[68] E4Tech. Review of technologies for gasification of biomass and wastes 2009.
[69] Bergman PCA, Boersma AR, Kiel JHA, Prins MJ, Ptasinski KJ, Janssen FJJG. Torrefaction for entrained-flow gasification of biomass 2004.
[70] Prins MJ, Ptasinski KJ, Janssen FJJG. More efficient biomass gasification via torrefaction. Energy 2006;31:3458–70.
[71] Yong YS, Rasid RA. Process simulation of hydrogen production through biomass gasification: introduction of torrefaction pre-treatment. Int J Hydrogen Energy 2022;47:42040–50.
[72] Svoboda K, Pohořelý M, Hartman M, Martinec J. Pretreatment and feeding of biomass for pressurized entrained flow gasification. Fuel Process. Technol. 2009;90:629–35.
[73] Harun NY, Afzal MT. Characteristics of product gas from torrefied biomass blends. Int. J. 2013;4.
[74] Chiesa P. Advanced technologies for syngas and hydrogen (H2) production from fossil-fuel feedstocks in power plants. In: Advanced power plant materials, design and technology. Elsevier; 2010. p. 383–411.
[75] Umeki K, Häggström G, Bach-Oller A, Kirtania K, Furusjö E. Reduction of tar and soot formation from entrained-flow gasification of woody biomass by alkali impregnation. Energy Fuel 2017;31:5104–10.
[76] Tapia A, Salgado S, Martín P, Villanueva F, García-Contreras R, Cabañas B. Chemical composition and heterogeneous reactivity of soot generated in the combustion of diesel and GTL (Gas-to-Liquid) fuels and amorphous carbon Printex U with NO2 and CF3COOH gases. Atmos Environ 2018;177:214–21.
[77] Göktepe B, Umeki K, Hazim A, Lundström TS, Gebart R. Soot reduction in an entrained flow gasifier of biomass by active dispersion of fuel particles. Fuel 2017;201:111–7.
[78] Kreutz TG, Larson ED, Elsido C, Martelli E, Greig C, Williams RH. Techno-economic prospects for producing Fischer-Tropsch jet fuel and electricity from lignite and woody biomass with CO2 capture for EOR. Appl Energy 2020;279:115841.
[79] Martín MM. Industrial chemical process analysis and design. Elsevier; 2016.
[80] Ramzan N, Rizwan M, Zaman M, Adnan M, Ullah A, Gungor A, et al. Pre-combustion carbon dioxide capture: a thermo-economic comparison for dual-stage Selexol process and combined Sulfinol-Selexol process. Int J Energy Res 2022;46:23775–95.
[81] Ahn H, Kapetaki Z, Brandani P, Brandani S. Process simulation of a dual-stage Selexol unit for pre-combustion carbon capture at an IGCC power plant. Energy Procedia 2014;63:1751–5.
[82] Masters C. The Fischer-Tropsch Reaction. Advances in Organometallic Chemistry. Elsevier 1979;17:61–103.
[83] Kölbel H, Ralek M. The Fischer-Tropsch synthesis in the liquid phase. Catal Rev Sci Eng 1980;21:225–74.
[84] Lin Q, Cheng M, Zhang K, Li W, Wu P, Chang H, et al. Development of an Iron-Based Fischer—Tropsch Catalyst with High Attrition Resistance and Stability for Industrial Application. Catalysts 2021;11:908.
[85] Steynberg AP, Dry ME, Davis BH, Breman BB. Fischer-tropsch reactors. Stud Surf Sci Catal 2004;152:64–195.
[86] Ail SS, Dasappa S. Biomass to liquid transportation fuel via Fischer Tropsch synthesis–Technology review and current scenario. Renew. Sustain. Energy Rev. 2016;58:267–86.
[87] Collis J, Duch K, Schomäcker R. Techno-economic assessment of jet fuel production using the Fischer-Tropsch process from steel mill gas. Front Energy Res 2022;10.
[88] Martín M, Grossmann IE. Process Optimization of FT-Diesel Production from Lignocellulosic Switchgrass. Ind Eng Chem Res 2011;50:13485–99. https://doi.org/10.1021/ie201261t.
[89] Botes FG, Dancuart LP, Nel HG, Steynberg AP, Vogel AP, Breman BB, et al. Middle distillate fuel production from synthesis gas via the Fischer-Tropsch process. Advances in clean hydrocarbon fuel processing. Elsevier 2011:329–62.
[90] Amaral F, Santos A, Calixto E, Pessoa F, Santana D. Exergetic Evaluation of an Ethylene Refrigeration Cycle. Energies (Basel) 2020;13:3753.

[91] Van der Westhuizen R, Potgieter H, Prinsloo N, De Villiers A, Sandra P. Fractionation by liquid chromatography combined with comprehensive two-dimensional gas chromatography–mass spectrometry for analysis of cyclics in oligomerisation products of Fischer-Tropsch derived light alkenes. J Chromatogr A 2011;1218:3173–9.
[92] De Klerk A. Aviation turbine fuels through the Fischer-Tropsch process. Biofuels for aviation: Elsevier; 2016. p. 241–59.
[93] Al-Kinany MC, Al-Drees SA, Al-Megren HA, Alshihri SM, Alghilan EA, Al-Shehri FA, et al. High-quality fuel distillates produced from oligomerization of light olefin over supported phosphoric acid on H-Zeolite-Y. Appl Petrochem Res 2019;9:35–45.
[94] Tomasek S, Lonyi F, Valyon J, Wollmann A, Hancsók J. Hydrocracking of Fischer-Tropsch Paraffin Mixtures over Strong Acid Bifunctional Catalysts to Engine Fuels. ACS Omega 2020;5:26413–20.
[95] Gamba S, Pellegrini LA, Calemma V, Gambaro C. Liquid fuels from Fischer-Tropsch wax hydrocracking: isomer distribution. Catal Today 2010;156:58–64.
[96] Calemma V, Gambaro C, Parker Jr WO, Carbone R, Giardino R, Scorletti P. Middle distillates from hydrocracking of FT waxes: composition, characteristics and emission properties. Catal Today 2010;149:40–6.
[97] Tepelus A, Dragomir RE, Rosca P. Sustainable aviation fuel from hydroconversion of safflower oil over NiMo/Al2O3 and Pt-ZrO2/Al2O3 catalysts. React. Kinet. Mech. Catal. 2022;135:1503–22.
[98] Bechtel. Aspen Process Flowsheet Simulation Model of a Battelle Biomass-Based Gasification. Fischer-Tropsch Liquefaction and Combined-Cycle Power Plant 1998.
[99] Aminov RZ, Moskalenko AB, Kozhevnikov AI. Optimal gas turbine inlet temperature for cyclic operation. J Phys Conf Ser, vol. 1111, IOP Publishing; 2018, p. 012046.
[100] González-Vázquez MP, Rubiera F, Pevida C, Pio DT, Tarelho LAC. Thermodynamic analysis of biomass gasification using aspen plus: comparison of stoichiometric and non-stoichiometric models. Energies (Basel) 2021;14:189.
[101] Martín MM. Introduction to software for chemical engineers. (2nd ed.). CRC Press; 2019.
[102] Mills KC, Rhine JM. The measurement and estimation of the physical properties of slags formed during coal gasification: 1. Properties relevant to fluid flow Fuel 1989;68:193–200.
[103] Dagle RA, Karim A, Li G, Su Y, King DL. Syngas conditioning. Fuel Cells: Technologies for Fuel Processing, Elsevier; 2011. p. 361–408.
[104] Meng L, Tsuru T. Microporous Silica Membrane Reactors. Current Trends and Future Developments on (Bio-) Membranes, Elsevier 2019:127–56.
[105] Li P, Yuan Z, Eden MR. A comparative study of Fischer-Tropsch synthesis for liquid transportation fuels production from biomass. Computer Aided Chemical Engineering, vol. 38, Elsevier; 2016, p. 2025–30.
[106] Zhang Y, Sunarso J, Liu S, Wang R. Current status and development of membranes for CO2/CH4 separation: a review. Int. J. Greenhouse Gas Control 2013;12:84–107.
[107] Ion D, Codrut PD. Efficiency assessment of condensing steam turbine. Advances in Environment, Ecosystems and Sustainable. Tourism 2013:203e208.
[108] Field RP, Brasington R. Baseline flowsheet model for IGCC with carbon capture. Ind Eng Chem Res 2011;50:11306–12.
[109] Finnveden G, Potting J. Life cycle assessment. Encyclopedia of. Toxicology 2014:74–7.
[110] JRC. ILCD Handbook - International Reference Life Cycle Data System. 2010.
[111] Djomo SN, El Kasmioui O, De Groote T, Broeckx LS, Verlinden MS, Berhongaray G, et al. Energy and climate benefits of bioelectricity from low-input short rotation woody crops on agricultural land over a two-year rotation. Appl Energy 2013;111:862–70.
[112] García-Freites S, Gough C, Röder M. The greenhouse gas removal potential of bioenergy with carbon capture and storage (BECCS) to support the UK's net-zero emission target. Biomass Bioenergy 2021;151:106164.
[113] Blakey S, Wilson CW, Farmery M, Midgley R. Fuel effects on range versus payload for modern jet aircraft. The Aeronautical Journal 2011;115:627–34.
[114] Airlines-Inform. Airbus A330-300 2023. https://www.airlines-inform.com/commercial-aircraft/airbus-a330-300.html (accessed April 12, 2023).
[115] de Klerk A, Maitlis PM. What Can We Do with Fischer-Tropsch Products? Greener Fischer-Tropsch Processes for Fuels and Feedstocks 2013:81–105.
[116] Ebrahimi P, Kumar A, Khraisheh M. A review of recent advances in water-gas shift catalysis for hydrogen production. Emergent Mater 2020;3:881–917.
[117] Mendes D, Garcia H, Silva VB, Mendes A, Madeira LM. Comparison of nanosized gold-based and copper-based catalysts for the low-temperature water– gas shift reaction. Ind Eng Chem Res 2009;48:430–9.
[118] Tavares M, Westphalen G, Ribeiro A, de Almeida JM, Romano PN, Sousa-Aguiar EF. Modified fischer-tropsch synthesis: a review of highly selective catalysts for yielding olefins and higher hydrocarbons. Frontiers. Nanotechnology 2022;4:978358.
[119] Prinsloo NM. Preparation of a solid phosphoric acid catalyst from low-quality kieselguhr parameters controlling catalyst quality and performance. Ind Eng Chem Res 2007;46:7838–43.
[120] Yang M, Zhang L, Wang G, Chen Z, Han J, Gao C, et al. Fischer-Tropsch wax catalytic cracking for the production of low olefin and high octane number gasoline: experiment and molecular level kinetic modeling study. Fuel 2021;303:121226.
[121] ICAO. ICAO carbon emissions calculation methodology 2018.
[122] de Klerk A. Fischer–tropsch process. Kirk-Othmer Encycl. Chem. Technol. 2013:1–20.
[123] Moser K, Wopienka E, Pfeifer C, Schwarz M, Sedlmayer I, Haslinger W. Screw reactors and rotary kilns in biochar production–A comparative review. J Anal Appl Pyrolysis 2023;106112.
[124] DeWitt MJ, Corporan E, Graham J, Minus D. Effects of aromatic type and concentration in Fischer– Tropsch fuel on emissions production and material compatibility. Energy Fuel 2008;22:2411–8.
[125] Faber J, Király J, Lee D, Owen B, O'Leary A. Potential for reducing aviation non-CO2 emissions through cleaner jet fuel. Delft: CE Delft; 2022.
[126] Zschocke A, Scheuermann S, Ortner J. High Biofuel Blends in Aviation (HBBA): ENER/C2/2012/420-1 Final Report. Deutsche Lufthansa; 2012.
[127] Jiang J, Feng X, Yang M, Wang Y. Comparative technoeconomic analysis and life cycle assessment of aromatics production from methanol and naphtha. J Clean Prod 2020;277:123525.
[128] Liu Y, Li G, Chen Z, Shen Y, Zhang H, Wang S, et al. Comprehensive analysis of environmental impacts and energy consumption of biomass-to-methanol and coal-to-methanol via life cycle assessment. Energy 2020;204:117961.
[129] Nugroho YK, Zhu L, Heavey C. Building an agent-based techno-economic assessment coupled with life cycle assessment of biomass to methanol supply chains. Appl Energy 2022;309:118449.
[130] Li J, Zhang Y, Yang Y, Zhang X, Zheng Y, Qian Q, et al. Comparative resource-environment-economy assessment of coal-and oil-based aromatics production. Resour. Policy 2022;77:102629.
[131] Argonne. The Greenhouse gases, Regulated Emissions, and Energy use in Technologies (GREET)Model. 2023.
[132] LBST. E3Database 2006.
[133] Elgowainy A, Han J, Wang M, Carter N, Stratton R, Hileman J, et al. Life-cycle analysis of alternative aviation fuels in GREET. Argonne National Lab.(ANL), Argonne, IL (United States); 2012.
[134] Boehm RC, Yang Z, Bell DC, Feldhausen J, Heyne JS. Lower heating value of jet fuel from hydrocarbon class concentration data and thermo-chemical reference data: an uncertainty quantification. Fuel 2022;311:122542.
[135] Egbumokei C. Energy use: fossil fuels by fuel type. 2023.
[136] EIA. Country Analysis Executive Summary: United Kingdom. 2022.
[137] Climate Change Committee. The sixth carbon budget-Aviation 2020.
[138] DfT. Jet Zero Strategy. Delivering net zero aviation by 2050. 2022.
[139] UK Government. Carbon Budget Delivery Plan. 2023.
[140] Boucher O, Borella A, Gasser T, Hauglustaine D. On the contribution of global aviation to the CO2 radiative forcing of climate. Atmos Environ 2021;267:118762.
[141] Schripp T, Anderson BE, Bauder U, Rauch B, Corbin JC, Smallwood GJ, et al. Aircraft engine particulate matter emissions from sustainable aviation fuels: results from ground-based measurements during the NASA/DLR campaign ECLIF2/ND-MAX. Fuel 2022;325:124764.
[142] Matthes S, Lim L, Burkhardt U, Dahlmann K, Dietmüller S, Grewe V, et al. Mitigation of non-CO2 aviation's climate impact by changing cruise altitudes. Aerospace 2021;8:36.
[143] Rizescu C, Sun C, Popescu I, Urdă A, Da Costa P, Marcu I-C. Hydrodeoxygenation of benzyl alcohol on transition-metal-containing mixed oxides catalysts derived from layered double hydroxide precursors. Catal Today 2021;366:235–44.
[144] Sakoda K, Yamaguchi S, Mitsudome T, Mizugaki T. Selective Hydrodeoxygenation of Esters to Unsymmetrical Ethers over a Zirconium Oxide-Supported Pt–Mo Catalyst. JACS Au 2022;2:665–72.
[145] Kuchinskaya TS, Mamian LG, Kniazeva MI. Hydrodeoxygenation of Diphenyl Ether over an In Situ NiMoS Catalyst. Pet. Chem. 2021;61:1124–30.
[146] Di Sanzo FP, Lane JL, Bergquist PM, Mooney SA, Wu BG. Determination of total oxygenates in Fischer-Tropsch liquid products. J Chromatogr A 1983;281:101–8.
[147] BEIS. Greenhouse gas reporting: conversion factors 2022. 2022.
[148] Real Guimarães H, Marcon Bressanin J, Lopes Motta I, Ferreira Chagas M, Colling Klein B, Bonomi A, et al. Decentralization of sustainable aviation fuel production in Brazil through Biomass-to-Liquids routes: a techno-economic and environmental evaluation. Energy Convers Manag. 2023;276:116547. https://doi.org/10.1016/j.enconman.2022.116547.
[149] M. Brandao i Canals LM, Clift R. Soil organic carbon changes in the cultivation of energy crops: Implications for GHG balances and soil quality for use in LCA Biomass Bioenergy 35 2011 2323 2336.